

THE DISTANCE OF THE LOCAL-GROUP GALAXY IC 1613 OBTAINED FROM BAADE'S WORK ON ITS STELLAR CONTENT*

ALLAN SANDAGE

Hale Observatories, Carnegie Institution of Washington,
 California Institute of Technology

Received 1970 December 24

ABSTRACT

Fifty-nine variables were found by Baade over the face of IC 1613 from a series of plates taken with the 100-inch reflector from 1929 to 1937. Of these, thirty-seven are definite Cepheids ranging in period from 146 days to 2 days, four are probable Cepheids, thirteen are irregular, one is a probable SRC, one is an eclipsing binary, and three are of unknown type.

Photometry depends on a photoelectric sequence of thirty-eight stars measured with the 200-inch reflector in the interval $11.6 \leq B \leq 21.7$. Magnitudes of 279 secondary standards used for the variables have been determined relative to the basic sequence. The values are listed in the Appendix.

Two interpretations of the period-luminosity relation are given for the Cepheids. The apparent blue modulus is $(m - M)_{AB} = 24.55$ as found from the most recent calibration of the P-L relation. A reddening of $E(B - V) \simeq 0.03$ gives the true modulus as $(m - M)_0 = 24.43$. The integrated absolute magnitude of IC 1613 is $M_B = -14.45$.

The brightest blue supergiant is star 22A with $M_B = -7.55$. The brightest red supergiant is the irregular red variable V42 with $M_B = -6.05$, or $M_V \simeq -8.0$ if $B = V$ is assumed to be 2.0. The largest H II region has a linear size of 167 pc. These absolute magnitudes and linear dimensions are much smaller than corresponding values in intrinsically brighter late-type galaxies.

The total extent of the Population II component of IC 1613 is 25'0 by 20'3, or 5600 by 4500 pc. The Population I component covers a region only half these dimensions.

I. INTRODUCTION

The galaxy IC 1613 [$\alpha_{1950} = 1^{\text{h}}02^{\text{m}}16^{\text{s}}.1$, $\delta_{1950} = +1^{\circ}52'29''$; $l^{\text{II}} = 130^{\circ}$, $b^{\text{II}} = -61^{\circ}$] was discovered by Wolf (1906) with the Bruce 16-inch refractor at Heidelberg. Baade (1928), using plates taken with the Bergedorf 40-inch reflector, classified it as a Magellanic-Cloud-type galaxy. From its resolution into individual stars at $m_{\text{pg}} \simeq 17$ mag, Baade concluded that the system was a member of the Local Group with a distance similar to that of NGC 6822 (Hubble 1925).

A series of plates was taken by Hubble with the 100-inch reflector from 1929 to 1932, after which Baade began his long study of the galaxy with the use of the 60-, 100-, and 200-inch reflectors. Baade's extensive results, principally on the variable stars, were never published, probably because of his reluctance to leave the problem in the face of uncertainties in the magnitude scale.

Between 1932 and 1955 three separate magnitude systems were carried. The first was based on the Seares scales (Seares, Kapteyn, and van Rhijn 1930) in SA 68, as extended by Baade to fainter magnitudes by photographic methods (exposure ratios, and neutral half-filters). The system was revised in 1939 by Baade's new work in SA 68 (Baade 1944), and again in 1955 by photographic transfers to Stebbins, Whitford, and Johnson (1950) photoelectric sequence in SA 68, as supplemented by Baum's unpublished extension to fainter magnitudes in this area.

Baade was not satisfied with the magnitude scale even after 1955 because of the very shallow slope for his Cepheid period-luminosity (P-L) relation. It seemed desirable to check this slope by photoelectric measurements of some of the sequence stars in IC 1613 directly. At Baade's request, this direct calibration was begun at the 200-inch in 1958

* With an Appendix on the adopted magnitude system by A. Sandage, Basil Katem, and Ann Hearn Matthews.

and was completed in 1963. Thirty-eight stars, measured in the magnitude interval $11.6 \leq B \leq 21.7$, formed the basis for transforming all secondary-sequence stars to the photoelectric system. The secondary-sequence reduction was made by Basil Katem, who used photographic iris photometry for all such stars which had been measured earlier by Mrs. Ann Hearn Matthews under Baade's direction. Details of the magnitude system for the thirty-eight photoelectric standards and the 279 secondary-sequence stars are given in the Appendix.

With each sequence calibrated, Baade's Argelander estimates for each variable were transformed to the B system, and all reductions of the light curves were made anew. The result of the work is discussed in this paper.

Baade's death in 1960 occurred while the new calibration was in progress, and before the final P-L relation was available. Baade's extensive series of plates, his discovery of the variables, choice of the sequence stars near each variable, period determination, and his intensity estimates form the basis of the present discussion. The photoelectric sequence, the reduction to the final magnitude system, and the analysis of the results are new. Baade cannot be held responsible for such errors as may yet be present in the adopted sequences, or for the necessarily tentative conclusions contained in the remaining sections.

II. PURPOSE

Why is IC 1613 so important? This galaxy is the faintest member of the Local Group [$M_B(\text{total}) \simeq -14.6$] among those which contain Cepheids. It is highly resolved into bright OBAF stars, it has well-defined H II regions, and the red supergiants are clearly visible. Once its distance modulus is known, the galaxy provides the low-luminosity anchor for calibrations of the size of H II regions, the M_B of the brightest blue stars, and the M_v of the brightest red stars as a function of galaxian luminosity class—calibrations which are first steps in a new determination of the Hubble constant.

But Baade's motivations were different. IC 1613 appears to have negligible internal absorption (many faint background galaxies appear over the entire face). Furthermore, the galactic absorption is small [$E(B - V) \lesssim 0.03$ from data in the Appendix], and its gradient over the face of the galaxy must be small or negligible. This galaxy is, therefore, one of the few members of the Local Group where the shape of the Cepheid P-L relation and the intrinsic dispersion about the ridge line are not affected by variations of the absorption. The hope of determining this dispersion is the reason Baade took such meticulous steps to insure the homogeneity of the magnitude sequences. Although the present material is not suited to find this dispersion for reasons discussed in § IV, the importance of IC 1613 as a fundamental calibrator remains crucial in the wider context of the Hubble constant. The primary purpose of the present work is, then, to obtain the distance.

III. THE VARIABLES

a) *Discovery*

A total of 106 plates of adequate quality were taken with either the 60-inch or the 100-inch reflector between 1929 and 1937, mostly by Baade, but a few were taken by Hubble, Duncan, and van Maanen. All plates were blue-sensitive, and were exposed without filters with exposure times ranging generally between 1 and 2 hours.

Hubble had blinked early plates of the series and discovered the Cepheids now labeled V16 and V18. From the same series, Mayall found variables 2 and 19. Baade blinked thirty-four plate pairs from the sample and gave numbers to a total of fifty-seven stars, of which numbers 4, 5, 33, and 35 later proved to be nonvariable. Six additional stars (V58–V63) were found in later comparisons, giving a total of fifty-nine confirmed variables. A discovery record was kept, from which the completeness of the search can be estimated by the method of van Gent (1933) (see also Plaut 1964). Analysis led Baade to conclude that a total of seventy-one variables may be present to the working

limit of excellent 100-inch plates ($B = 22.2$, cf § III*d*), a conclusion which shows that the present sample is about 83 percent complete.¹

b) Identification

The fifty-nine variables are identified in Figure 1 (Plate 1). Also marked are the thirty-eight primary photoelectric standards listed in the Appendix. As an aid for future work, the sequence stars used for each variable are identified on the large-scale reproductions of the four quadrants in Figures 2–6 (Plates 2–6).

Table 1, to be used with Figures 2–6, is a finding directory for the fifty-nine variables and their sequences. The type of star is listed in column (2) (δ for Cepheid, SRc for the variable V19, RI for red irregular, BI for the one blue irregular V44, I for intermediate-color irregular, and E for the eclipsing variable). Of the fifty-nine stars, thirty-seven are definite Cepheids, four are probable Cepheids, twelve are irregular red variables, one is a blue irregular, one is an eclipsing variable, one is a semiregular long-period

TABLE 1
DIRECTORY OF THE FIFTY-NINE VARIABLES IN IC 1613

No. (1)	Type (2)	Quadrant (3)	Status (4)	No. (1)	Type (2)	Quadrant (3)	Status (4)
1.....	δ	SE	F	34.....	δ	SW	F
2.....	δ	SW	F	35.....	δ	NW	TBD (3 ^d)
3.....	δ	SE	F	36.....	δ	NW	TBD (2 ^d 4)
6.....	δ	NW	F	37.....	δ	SW	F
7.....	δ	NE	TBD (7 ^d 1)	38.....	RI	NE2	F
8.....	?	NE2	TBD	39.....	δ	NE2	F
9.....	δ	NE	F	40.....	RI	NE	TBD
10.....	δ	NE	F	41.....	δ ?	NW	TBD
11.....	δ	NW	F	42.....	RI	NW	F
12.....	δ	NE2	F	43.....	RI	NE2	F
13.....	δ	NE	F	44.....	BI	SW	F
14.....	δ	SE	F	45.....	RI	NE	F
15.....	δ	SW	F	46.....	δ ?	NW	TBD
16.....	δ	NW	F	47.....	δ	SE	TBD (29 ^d 3)
17.....	δ	NW	F	48.....	δ ?	SW	TBD (2 ^d 666)
18.....	δ	NE	F	49.....	δ	NE	TBD (8 ^d 84)
19.....	SRc	SW	F	50.....	RI	SW	F
20.....	δ	SE	F	51.....	?	SW	TBD
21.....	RI	NE2	F	52.....	I	NE	F
22.....	δ	NE2	F	53.....	δ	NE	TBD (3 ^d 85)
23.....	RI	SE	F	54.....	δ	NE	TBD (4 ^d)
24.....	δ	NW	F	56.....	RI	NE2	F
25.....	δ	SW	F	57.....	δ ?	NW	TBD
26.....	δ	SW	F	58.....	I?	NE	TBD
27.....	δ	SW	F	59.....	δ	SW	TBD (2 ^d)
28.....	δ	SW	TBD (2 ^d 7?)	60.....	δ	SW	TBD (2 ^d)
29.....	δ	NE	F	61.....	δ	SW	TBD (3 ^d 99)
30.....	δ	NW	F	62.....	δ	SW	TBD (3 ^d)
31.....	E	NE	F	63.....	?	SW	TBD
32.....	RI	NE	F				

NOTE.—See text for explanations of cols. (2) and (4).

¹ Tabulations were separately kept for plates in two quality groups: (a) excellent to very good and (b) average plates. The mean discovery rate was 13.1 variables per pair of quality (a), and 6.7 variables per pair of quality (b). Baade notes "this shows how vital it is to have plates taken under the very best seeing conditions for finding variables in extragalactic systems of the Local Group. Plates taken under average seeing conditions yield only half as many variables as the best plates. This is probably the reason that Hubble found only Cepheids with $P > 10^d$ in M31, M33, and NGC 6822."

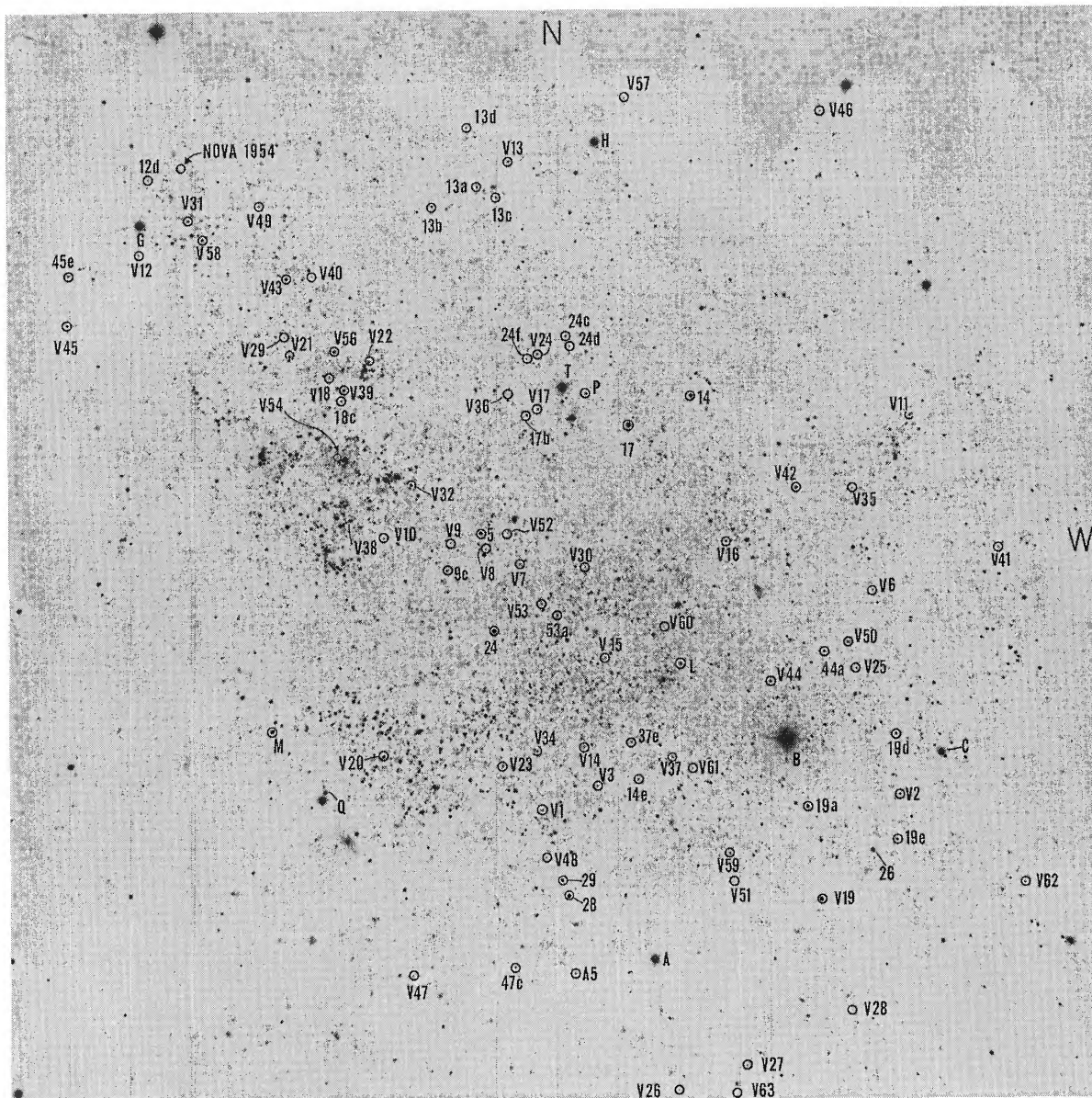


FIG. 1.—Identification chart for the 59 variables and 38 primary photoelectric standards. The variable star numbers are all preceded by the symbol V. All others have photoelectric magnitudes listed in Table A1 of the Appendix.

SANDAGE (*see* page 15)

PLATE 2

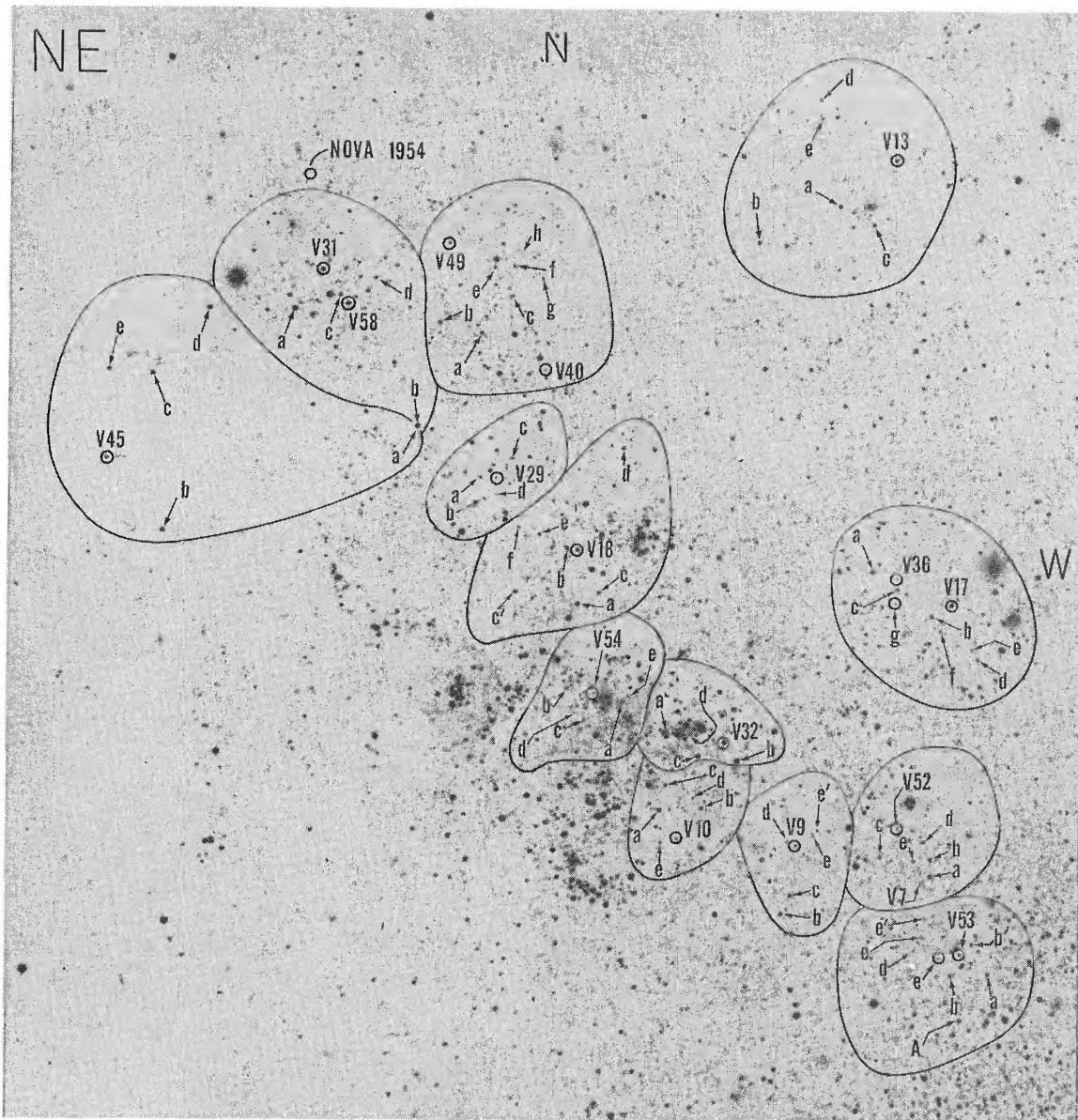


FIG. 2.—Identification chart for the variables and secondary sequence stars in the NE quadrant of IC 1613. Photograph is an enlargement from a 103a-O + GG13 plate taken with the Hale 200-inch telescope.

SANDAGE (see page 15)

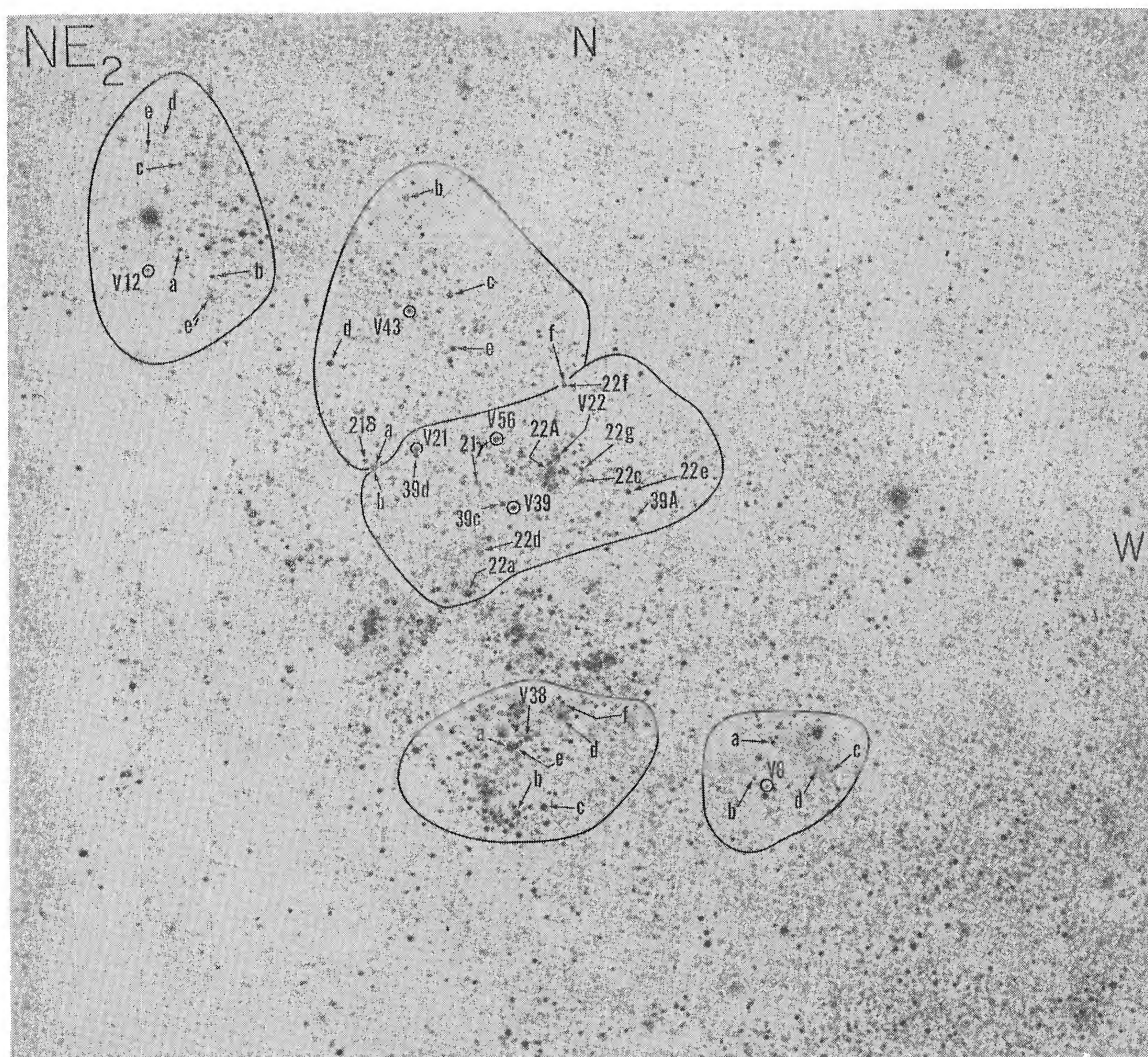


FIG. 3.—Same as Fig. 2 for additional stars in the NE quadrant
SANDAGE (see page 15)

PLATE 4

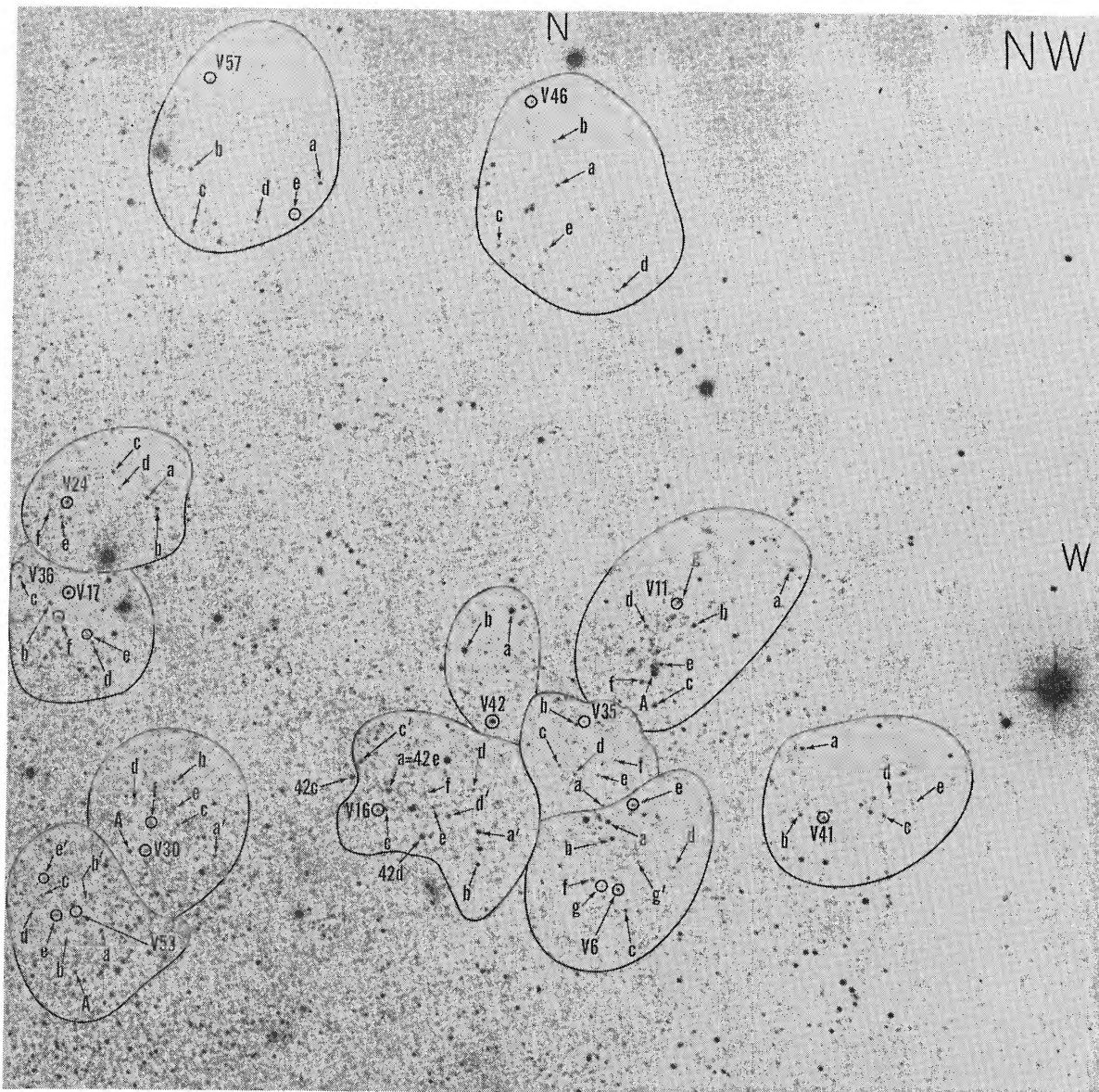


FIG. 4.—Same as Fig. 2 for the NW quadrant

SANDAGE (see page 15)

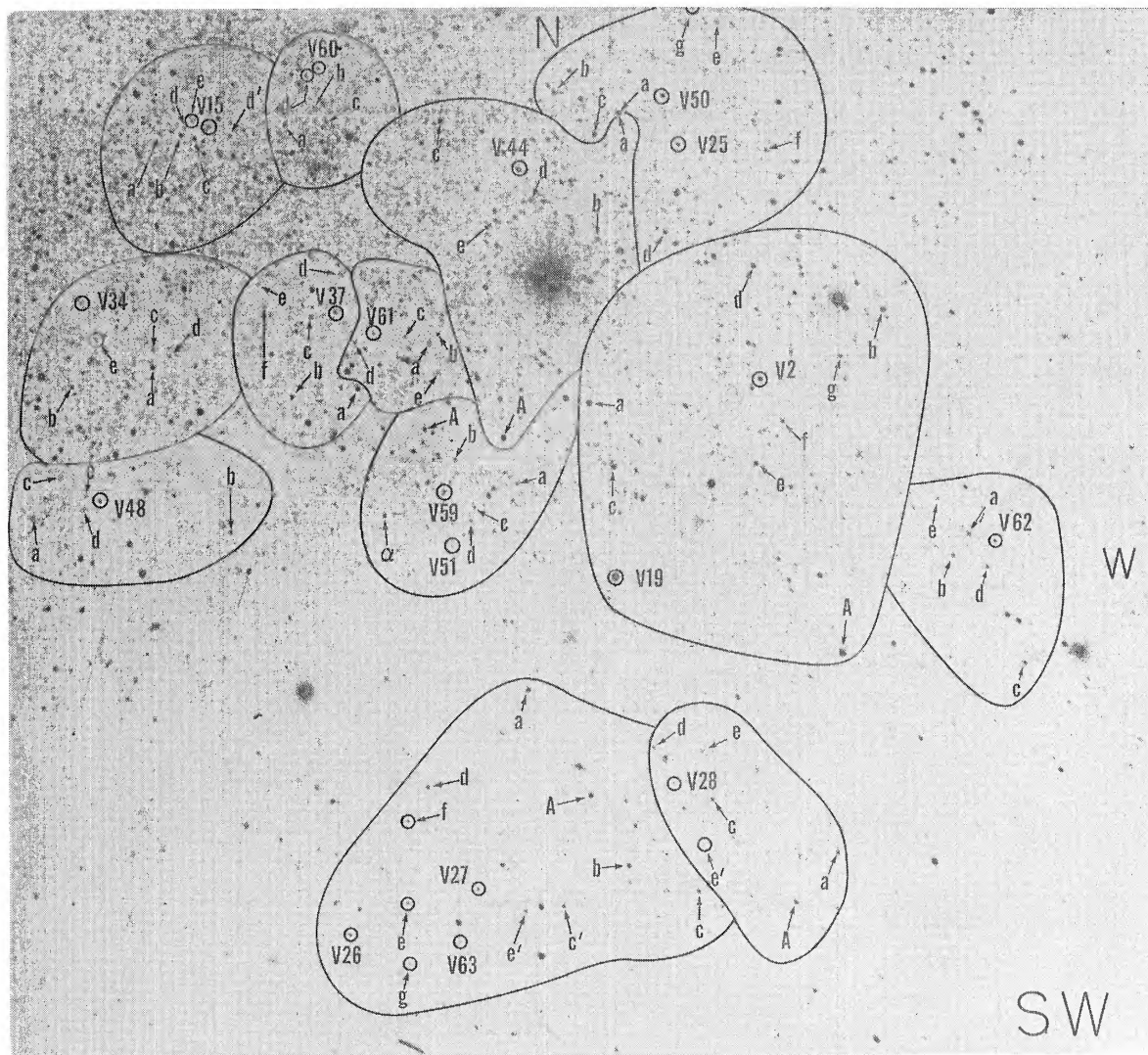


FIG. 5.—Same as Fig. 2 for the SW quadrant

SANDAGE (see page 15)

PLATE 6

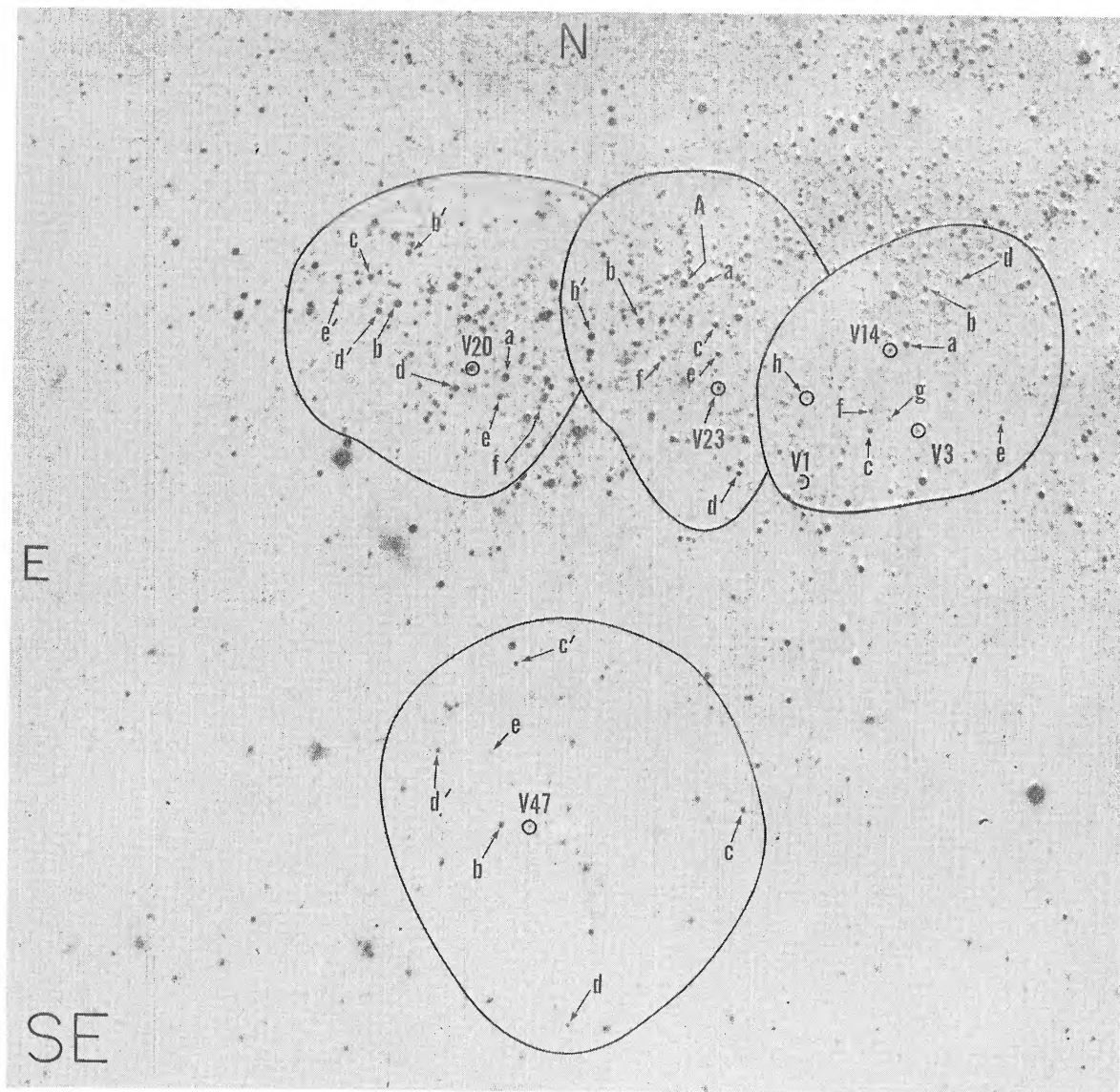


FIG. 6.—Same as Fig. 2 for the SE quadrant

SANDAGE (see page 15)

variable, and three are of unknown type. The chart name where each variable and its sequence is identified is listed in column (3), and the status of the work is in column (4) (F for finished, TBD for to be done). Baade completed preliminary work on some of the TBD stars, and his suggested periods are listed. *Work was finished on only those variables which remained above plate limit at minimum.* The TBD stars are generally very faint and are not seen during part of their light curve. This restriction causes a bias in the P-L plot below $P \simeq 3$ days which, in the presence of intrinsic dispersion, must be accounted for in determining the distance modulus (§ IV).

c) Photometry

Baade made eye estimates of all variables, relative to the sequence stars, by the Argelander method (i.e., if the sequence stars are labeled a , b , etc., in order of image size, and if the image size of a variable appears to be, say, 0.7 of the way from its sequence star a to b , its brightness is listed as $a7b$). The method proved to be of enormous advantage because changes in the magnitude system do not affect the estimates. Reduction to magnitudes can be made at any later time when new sequence values are available.

Two independent Argelander estimates of each variable were made on each plate, separated by a suitable time interval such that the memory was lost between. Baade had reduced his estimates first to the 1937 magnitude system and later to that of 1939. I reworked the reduction using the magnitudes adopted in the Appendix, Table A2, but the procedure was not straightforward due to the following circumstance.

Between 1929 and 1934 the telescope mirrors had been coated with silver, freshly applied every 6 months. But in early 1935 John Strong successfully deposited aluminum coats on both the 60-inch and 100-inch mirrors, causing the ultraviolet transmission to increase greatly. This led to an abrupt change in the color system. However, the IC 1613 plates had been taken without filters, and the increased ultraviolet sensitivity had an immediate effect, though it was discovered only after the 1935–1937 plates had been reduced and compared with the earlier series. The standard stars are predominantly blue, being main-sequence members of IC 1613 brighter than $M_B \simeq -2.5$. But the Cepheids are red. With aluminum-coated mirrors, more ultraviolet light is added to the images of the standard stars than to Cepheids, making them brighter relative to Cepheids; i.e., a color equation exists. What Baade found was: if the adopted magnitudes of the standards are kept constant, *all Cepheids appeared fainter after 1935 than before that date.*²

Because colors of the standards were not known, so that the plates could not be reduced with a color equation in the normal manner, Baade adopted the following procedure. Each sequence was estimated internally relative to itself (e.g., star b of the sequence was estimated relative to stars a and c , such as, say, $b = abc$; c was estimated relative to b and d , such as $c = b3d$; etc., down the line). This was done for both the aluminum and the silver systems. By adopting a zero-point magnitude for the endpoint star a and the faintest star, it was possible to find smoothed magnitudes for the other sequence members, *on the color system of the plates*. These magnitudes, of course, differed between the aluminum and silver systems by the (unknown) color equation. They also differed in an absolute sense because the endpoint stars (the brightest and faintest) themselves have a color equation relative to the Cepheids. Hence, final zero-point adjustments were made for each Cepheid separately by forcing the segments of its own light curves to coincide for the two intervals from 1929 to 1934 and from 1935 to 1937.

I encountered the same difficulties in the new magnitude system of the Appendix. I proceeded in the same way, using Baade's individual "homogenization" equations (i.e., $b = anc$, $c = bmd$, $d = cqe$, etc., where n , m , q , etc., are the observed size ratios)

² Plates taken after 1937 were "corrected to the silver system" by adding a minus UV filter (Schott WG2), but this did not alleviate the problem between 1935 and 1937.

for each sequence for both the silver and aluminum series, and adopting the endpoint magnitudes for the brightest and faintest star as in the Appendix. The additional proviso was made that the derived magnitudes for stars b, c, d, \dots , on the silver system should agree in the mean with those in the Appendix. This provides a check and a smoothing of Baade's homogenization equations because silver mirrors with blue plates without filter closely imitate the B photometric system of Table A2 (Appendix).

Comparison between the "silver" and "aluminum" light curves then provided zero-point adjustments to the final *silver* system which was adopted as the best approximation to B . It is, however, expected that a small color equation still exists, depending in each case on (1) the difference in color index between the sequence star and the Cepheid and (2) the exact difference in effective wavelength between a bare silver mirror with 103a-O plates and the B photoelectric system. Although small, the effect must be considered in a future extension of the present work when colors of the Cepheids are derived, if B values of this paper are used.

A second method was used to check all values. Baade had listed the reductions (corrected to the silver system) of all variables to his 1939 magnitude system. There were also tables of his 1939 silver magnitudes for all sequence stars. Comparison of these with the B values of Table A1 (Appendix) gave a *mean* correction curve $m_{pg}(1939) - B = f[m(1939)]$ from which the 1939 magnitudes could be reduced to the new photoelectric system.³ Katem undertook this parallel *mean* reduction of the Cepheids. The results are not tabulated since they suffer in principle from the uncertainty mentioned in footnote 3, but the agreement with the more detailed reduction is satisfactory in the mean.

Final adopted magnitudes of the Cepheids are listed in Table 2. This table lists phases of the variables calculated by using the epoch of maximum and the period listed later in Table 6. All dates are Julian Day reduced to Greenwich Mean Time, but not to the Sun because the periods of the variables are long compared with the light-time across the Earth's orbit.

d) *The Cepheids*

Light curves for twenty-four of the Cepheids are shown in Figures 7 and 8, displayed in order of period. To test if errors remain between the silver and aluminum systems, different symbols have been used: open circles are the silver system (1929–1934); filled circles are aluminum points (1935–1937) reduced to the silver system. The lack of systematic error appears to be quite satisfactory.

With the exception of a few Cepheids, the scatter in the light curves is close to that expected from the estimated probable error of ± 0.10 mag for a single entry in Table 2. This error was estimated from comparison of (1) the first and second estimates of intensity and (2) scatter in estimated magnitudes for several stars carried as variables but later shown to be constant.

Of the Cepheids, only V22 ($P = 146^d.35$) and one other needs special mention. V22 has an unusually long period and is the only Cepheid which does not repeat well. However, its period has remained constant over the observing interval, comprising 18 cycles, as shown by the lack of systematic trend in the observed minus computed epoch of maximum for ten well-observed maxima. The period of 146 days is abnormally long for a Cepheid. Known Cepheids with periods greater than 100 days include HV 1956 ($P = 210^d$) and HV 821 ($P = 127^d$) in the Small Magellanic Cloud, HV 2447 ($P = 118^d$) and HV 883 ($P = 134^d$) in the Large Magellanic Cloud, and H42 in M31 ($P = 176^d.7$, Baade and Swope 1965). V22 in IC 1613 is the Cepheid with the third longest

³ The disadvantage of the method was that Baade's (1939) m_{pg} for the sequence stars were based on his first attempt to tie all sequence stars together (by overlapping 100-inch plates taken with the 84-inch diaphragm to minimize coma effects). Baade later rehomogenized the sequence stars in 1955 by using Mrs. Matthews's measurements of 200-inch plates; the new material is the basis for Table A2, hence the new reduction is preferred.

TABLE 2
B MAGNITUDES FOR CEPHEIDS IN IC 1613

JD	Year	Plate	VI*	V2	V3	V6	V9	V10	V11	V12	V13	V14	V15	V16	V17
			Phase B	Phase B	Phase B	Phase B	Phase B	Phase B	Phase B	Phase B	Phase B	Phase B	Phase B	Phase B	Phase B
5829-986	1929	H1097H	0.799 20.93	0.457 20.28	0.712 21.46:	0.765 21.52	0.145 20.95	0.145 20.95	0.109 20.01	0.109 20.01	0.109 20.01	0.109 20.01	0.109 20.01	0.109 20.01	0.109 20.01
6211-762	1930	H1196H	0.172 21.10:	0.153 19.60	0.215 20.70	0.287 21.17	0.111 21.17	0.111 21.17	0.111 21.17	0.111 21.17	0.111 21.17	0.111 21.17	0.111 21.17	0.111 21.17	0.111 21.17
6269-792	"	H1198H	0.203 19.70	0.203 19.70	0.245 20.63	0.434 21.37	0.089 20.93	0.089 20.93	0.134 20.38	0.134 20.38	0.134 20.38	0.134 20.38	0.134 20.38	0.134 20.38	0.134 20.38
6304-642	"	H1199H	0.683 21.30	0.690 21.05	0.047 20.68	0.865 <21.30	0.000	0.000	0.000	0.000	0.000	0.000	0.000	0.000	0.000
6594-976	1931	H1324H	0.038 20.46:	0.066 19.52	0.464 21.30:	0.357 21.40	0.428 21.65	0.428 21.65	0.971 19.75	0.971 19.75	0.971 19.75	0.971 19.75	0.971 19.75	0.971 19.75	0.971 19.75
6619-781	"	H1325H	0.123 19.62	0.123 19.62	0.000	0.865 <21.30	0.000	0.000	0.000	0.000	0.000	0.000	0.000	0.000	0.000
6688-709	"	B5B	0.061 19.55	0.061 19.55	0.000	0.357 21.40	0.428 21.65	0.428 21.65	0.933 19.84	0.933 19.84	0.933 19.84	0.933 19.84	0.933 19.84	0.933 19.84	0.933 19.84
6925-960	1932	B1107B	0.790 21.24	0.173 19.68	0.931 20.87	0.246 21.32	0.745 21.41	0.745 21.41	0.000	0.000	0.000	0.000	0.000	0.000	0.000
6926-946	"	B1111B	0.966 20.46:	0.216 19.88	0.931 20.87	0.246 21.32	0.745 21.41	0.745 21.41	0.000	0.000	0.000	0.000	0.000	0.000	0.000
6956-944	"	B1188B	0.330 20.98	0.494 20.70	0.554 <21.45	0.798 21.78	0.367 21.51	0.367 21.51	0.016 19.70	0.016 19.70	0.016 19.70	0.016 19.70	0.016 19.70	0.016 19.70	0.016 19.70
6957-971	"	B1253B	0.514 21.45	0.538 20.71	0.814 22.12:	0.983 20.94:	0.620 21.41	0.620 21.41	0.055 19.74	0.055 19.74	0.055 19.74	0.055 19.74	0.055 19.74	0.055 19.74	0.055 19.74
6958-944	"	B1353B	0.688 21.38	0.579 20.95	0.058 21.16	0.158 21.28	0.858 21.59	0.858 21.59	0.093 19.82	0.093 19.82	0.093 19.82	0.093 19.82	0.093 19.82	0.093 19.82	0.093 19.82
6959-920	"	B1423B	0.863 21.29	0.621 20.90	0.305 21.68	0.333 21.44:	0.101 21.00	0.101 21.00	0.131 20.11	0.131 20.11	0.131 20.11	0.131 20.11	0.131 20.11	0.131 20.11	0.131 20.11
6984-807	"	B1463B	0.313 21.02:	0.682 20.94	0.172 20.83	0.394 21.32	0.421 21.17	0.421 21.17	0.101 19.89	0.101 19.89	0.101 19.89	0.101 19.89	0.101 19.89	0.101 19.89	0.101 19.89
6984-921	"	B1473B	0.333 21.06:	0.682 20.94	0.172 20.83	0.394 21.32	0.421 21.17	0.421 21.17	0.101 19.89	0.101 19.89	0.101 19.89	0.101 19.89	0.101 19.89	0.101 19.89	0.101 19.89
6982-898	"	B1474B	0.333 21.06:	0.682 20.94	0.172 20.83	0.394 21.32	0.421 21.17	0.421 21.17	0.101 19.89	0.101 19.89	0.101 19.89	0.101 19.89	0.101 19.89	0.101 19.89	0.101 19.89
6982-898	"	B1475B	0.333 21.06:	0.682 20.94	0.172 20.83	0.394 21.32	0.421 21.17	0.421 21.17	0.101 19.89	0.101 19.89	0.101 19.89	0.101 19.89	0.101 19.89	0.101 19.89	0.101 19.89
7007-764	"	B1545B	0.584 21.32:	0.770 20.75	0.101 21.36	0.167 21.14	0.490 21.51	0.490 21.51	0.139 20.12	0.139 20.12	0.139 20.12	0.139 20.12	0.139 20.12	0.139 20.12	0.139 20.12
7007-764	"	B1578B	0.418 21.34:	0.663 21.02	0.383 <21.45	0.923 21.62	0.868 21.65	0.868 21.65	0.177 20.25	0.177 20.25	0.177 20.25	0.177 20.25	0.177 20.25	0.177 20.25	0.177 20.25
7008-709	"	B1628B	0.431 21.38:	0.701 20.86	0.706 21.63	0.923 21.62	0.868 21.65	0.868 21.65	0.177 20.25	0.177 20.25	0.177 20.25	0.177 20.25	0.177 20.25	0.177 20.25	0.177 20.25
7008-760	"	B1633B	0.600 21.35:	0.704 20.95	0.602 22.16	0.713 21.62	0.101 21.10	0.101 21.10	0.027 19.80	0.027 19.80	0.027 19.80	0.027 19.80	0.027 19.80	0.027 19.80	0.027 19.80
7036-661	"	B1703B	0.586 21.12:	0.892 20.45	0.645 <21.90	0.091 20.94:	0.118 21.10	0.118 21.10	0.109 20.20	0.109 20.20	0.109 20.20	0.109 20.20	0.109 20.20	0.109 20.20	0.109 20.20
7039-714	"	B1723B	0.592 21.23	0.022 19.44	0.993 20.36	0.109 21.00	0.863 21.65	0.863 21.65	0.196 20.37	0.196 20.37	0.196 20.37	0.196 20.37	0.196 20.37	0.196 20.37	0.196 20.37
7064-656	"	B2468B	0.734 20.98	0.177 19.77	0.456 <21.5	0.348 21.39	0.327 21.34	0.327 21.34	0.000	0.000	0.000	0.000	0.000	0.000	0.000
7277-951	1933	B2505B	0.909 20.70	0.219 19.87	0.358 21.01	0.524 21.74	0.568 21.45	0.568 21.45	0.000	0.000	0.000	0.000	0.000	0.000	0.000
7278-928	"	B2753B	0.812 20.93	0.625 20.80	0.023 21.08	0.441 21.56	0.689 21.50	0.689 21.50	0.000	0.000	0.000	0.000	0.000	0.000	0.000
7335-851	"	B2783B	0.088 20.76:	0.644 20.95	0.048 20.90	0.728 21.76	0.571 21.45	0.571 21.45	0.000	0.000	0.000	0.000	0.000	0.000	0.000
7342-817	"	B2813B	0.334 21.04	0.941 19.87	0.804 <21.45	0.979 20.96:	0.285 21.45	0.285 21.45	0.989 19.76	0.989 19.76	0.989 19.76	0.989 19.76	0.989 19.76	0.989 19.76	0.989 19.76
7342-817	"	B2823B	0.382 21.17:	0.664 20.90	0.081 21.25	0.934 20.92	0.285 21.45	0.285 21.45	0.647 21.21	0.647 21.21	0.647 21.21	0.647 21.21	0.647 21.21	0.647 21.21	0.647 21.21
7359-863	"	B2923B	0.382 21.17:	0.664 20.90	0.081 21.25	0.934 20.92	0.285 21.45	0.285 21.45	0.647 21.21	0.647 21.21	0.647 21.21	0.647 21.21	0.647 21.21	0.647 21.21	0.647 21.21
7366-850	"	B2923B	0.382 21.17:	0.664 20.90	0.081 21.25	0.934 20.92	0.285 21.45	0.285 21.45	0.647 21.21	0.647 21.21	0.647 21.21	0.647 21.21	0.647 21.21	0.647 21.21	0.647 21.21
7391-749	"	B3063B	0.157 20.90:	0.865 19.34	0.683 21.65:	0.034 20.94:	0.477 21.38	0.477 21.38	0.921 20.03	0.921 20.03	0.921 20.03	0.921 20.03	0.921 20.03	0.921 20.03	0.921 20.03
7392-699	"	B3078B	0.254 20.51:	0.027 19.27	0.136 21.07	0.951 21.82:	0.553 21.41	0.553 21.41	0.924 19.89	0.924 19.89	0.924 19.89	0.924 19.89	0.924 19.89	0.924 19.89	0.924 19.89
7393-735	"	B3111B	0.719 21.32:	0.067 19.37	0.375 <21.5	0.106 20.88:	0.806 21.50	0.806 21.50	0.964 19.81	0.964 19.81	0.964 19.81	0.964 19.81	0.964 19.81	0.964 19.81	0.964 19.81
7417-670	"	B3117B	0.439 21.32:	0.111 19.42	0.635 22.14:	0.398 21.60	0.696 21.57	0.696 21.57	0.993 20.53	0.993 20.53	0.993 20.53	0.993 20.53	0.993 20.53	0.993 20.53	0.993 20.53
7449-645	"	B3277B	0.796 21.42:	0.494 20.37	0.668 22.03:	0.129 21.26:	0.561 20.86	0.561 20.86	0.208 20.20	0.208 20.20	0.208 20.20	0.208 20.20	0.208 20.20	0.208 20.20	0.208 20.20
7451-654	"	B3278B	0.045 20.51:	0.580 20.90	0.232 21.45	0.837 21.52	0.546 21.59	0.546 21.59	0.294 20.36	0.294 20.36	0.294 20.36	0.294 20.36	0.294 20.36	0.294 20.36	0.294 20.36
7659-978	"	B3998B	0.228 21.22:	0.502 20.70	0.988 21.06	0.022 21.03	0.546 21.59	0.546 21.59	0.334 20.41	0.334 20.41	0.334 20.41	0.334 20.41	0.334 20.41	0.334 20.41	0.334 20.41
7661-941	"	B4022B	0.401 21.31:	0.544 20.78	0.229 21.44	0.194 21.19:	0.782 21.36	0.782 21.36	0.371 20.45	0.371 20.45	0.371 20.45	0.371 20.45	0.371 20.45	0.371 20.45	0.371 20.45
7664-877	"	B4068B	0.502 21.43	0.521 20.90	0.013 20.93	0.307 21.29	0.423 21.62	0.423 21.62	0.307 20.35	0.307 20.35	0.307 20.35	0.307 20.35	0.307 20.35	0.307 20.35	0.307 20.35
7686-934	"	B372	0.000	0.000	0.000	0.000	0.000	0.000	0.000	0.000	0.000	0.000	0.000	0.000	0.000
7687-970	"	B377	0.000	0.000	0.000	0.000	0.000	0.000	0.000	0.000	0.000	0.000	0.000	0.000	0.000
7689-867	"	B4149B	0.394 21.31:	0.734 20.98	0.270 21.68	0.201 21.25	0.652 21.56	0.652 21.56	0.455 20.72	0.455 20.72	0.455 20.72	0.455 20.72	0.455 20.72	0.455 20.72	0.455 20.72
7689-954	"	B4153B	0.738 21.00	0.738 21.00	0.943 19.32	0.215 21.24	0.672 21.56	0.672 21.56	0.028 20.98	0.028 20.98	0.028 20.98	0.028 20.98	0.028 20.98	0.028 20.98	0.028 20.98
7691-882	"	HubbleA	0.820 20.90	0.820 20.90	0.000	0.000	0.000	0.000	0.000	0.000	0.000	0.000	0.000	0.000	0.000
7713-833	"	HubbleA	0.756 20.72	0.756 20.72	0.307 <21.45	0.476 21.29	0.545 21.28:	0.545 21.28:	0.000	0.000	0.000	0.000	0.000	0.000	0.000
7719-862	"	B366	0.970 19.26	0.970 19.26	0.011 20.50	0.497 21.38	0.146 21.60	0.146 21.60	0.385 20.35	0.385 20.35	0.385 20.35	0.385 20.35	0.385 20.35	0.385 20.35	0.385 20.35
7719-862	"	B366	0.014 19.21	0.014 19.21	0.000	0.000	0.000	0.000	0.000	0.000	0.000	0.000	0.000	0.000	0.000

Star VI is double. Magnitudes marked * designate plates where the variable is separated from the companion.

TABLE 2--Continued

ID	Plate	V18	V20	V22	V24	V25	V26	V27	V29	V30	V34	V37	V39	V31	V42
		Phase	Phase	Phase	Phase	Phase	Phase	Phase	Phase	Phase	Phase	Phase	Phase	Phase	B
5829-958	H1097E	0.785 21.12	0.440 20.09	0.773 18.76	0.878 21.37	0.273 20.40	0.959 21.27	0.839 21.46	0.164 21.58	0.164 21.58	0.142 21.00	0.410 21.00	0.837 19.80	0.882 20.13	19.33
6211-962	H1166R	0.028 20.27	0.546 20.50	0.384 19.90	0.525 21.52	0.744 21.24	0.959 21.27	0.839 21.46	0.634 21.97	0.634 21.97	0.142 21.00	0.180 20.72	0.138 19.61	0.930 20.14	18.68
6268-978	H1164E	0.485 21.23	0.900 19.99	0.773 19.78	0.952 20.50	0.912 20.64	0.730 <21.62	0.371 21.42	0.943 21.61	0.943 21.61	0.142 21.00	0.117 19.68	0.117 19.68	0.137 20.15	19.06
6269-792	H1194E	0.824 19.80	0.780 19.72	0.101 20.48	0.802 20.18	0.802 20.18	0.802 20.18	0.754 <21.62	0.381 21.47	0.381 21.47	0.142 21.00	0.152 19.75	0.403 20.12	0.403 20.12	19.31
6304-642	H1199E	0.667 21.12	0.755 20.55	0.017 17.87	0.269 21.36	0.826 21.36	0.894 21.53	0.754 <21.62	0.381 21.47	0.381 21.47	0.142 21.00	0.696 20.00	0.472 19.39	0.551 20.14	18.83
6594-976	H1394E	0.841 21.09	0.267 20.10	0.171 18.13	0.001 20.38	0.326 20.34	0.078 21.07	0.069 20.65	0.150 21.49	0.150 21.49	0.142 21.00	0.034 20.45	0.338 19.67	0.122 20.13	19.23
6619-761	H1398E	0.035 20.30	0.546 20.50	0.384 19.90	0.525 21.52	0.744 21.24	0.959 21.27	0.839 21.46	0.164 21.58	0.164 21.58	0.142 21.00	0.180 20.72	0.138 19.61	0.930 20.14	18.94
6695-709	B37	0.531 21.21	0.588 20.42	0.269 19.16	0.405 21.52	0.356 20.43	0.721 <21.62	0.139 20.63	0.861 21.91	0.861 21.91	0.142 21.00	0.117 19.68	0.117 19.68	0.137 20.15	18.80
6926-946	B111B	0.356 21.06	0.303 19.86	0.474 19.70	0.959 20.51	0.621 21.37	0.048 21.09	0.691 21.66	0.118 21.39	0.118 21.39	0.142 21.00	0.193 20.78	0.077 18.98	0.444 20.07	20.20
6956-944	B118B	0.418 21.26	0.328 19.93	0.482 19.63	0.733 <21.45	0.838 21.08	0.392 21.59	0.992 20.65	0.586 21.72	0.586 21.72	0.142 21.00	0.802 20.99	0.113 19.46	0.716 20.06	18.83
6958-944	B135B	0.477 21.31	0.351 20.08	0.488 19.90	0.295 21.25	0.838 21.08	0.392 21.59	0.992 20.65	0.586 21.72	0.586 21.72	0.142 21.00	0.802 20.99	0.113 19.46	0.716 20.06	18.83
6959-920	B142B	0.537 21.31	0.374 20.15	0.495 19.64	0.441 21.36	0.945 20.36	0.560 21.62	0.138 20.82	0.815 21.69	0.815 21.69	0.142 21.00	0.916 20.63	0.147 19.55	0.974 20.14	19.36
6984-807	B146B	0.051 20.35	0.968 19.06	0.665 19.28	0.132 20.58	0.647 21.45	0.838 21.50	0.875 21.39	0.899 21.94	0.899 21.94	0.142 21.00	0.980 20.74	0.422 18.93	0.825 20.04	19.38
6985-898	B151B	0.058 20.30	0.970 19.15	0.666 19.63	0.148 20.78	0.659 21.38	0.858 21.69	0.875 21.39	0.899 21.94	0.899 21.94	0.142 21.00	0.980 20.74	0.422 18.93	0.825 20.04	19.38
6985-898	B151B	0.117 20.70	0.994 19.15	0.672 19.70	0.158 20.96	0.765 21.31	0.826 21.07	0.875 21.39	0.899 21.94	0.899 21.94	0.142 21.00	0.980 20.74	0.422 18.93	0.825 20.04	19.38
6987-764	B152B	0.448 21.32	0.515 20.28	0.822 18.70	0.439 21.06	0.876 21.31	0.826 21.07	0.875 21.39	0.899 21.94	0.899 21.94	0.142 21.00	0.980 20.74	0.422 18.93	0.825 20.04	19.38
7007-836	B158B	0.452 21.32	0.517 20.27	0.822 18.70	0.535 21.48	0.876 21.31	0.826 21.07	0.875 21.39	0.899 21.94	0.899 21.94	0.142 21.00	0.980 20.74	0.422 18.93	0.825 20.04	19.38
7008-780	B163B	0.505 21.32	0.537 20.42	0.828 18.66	0.547 21.38	0.876 21.31	0.826 21.07	0.875 21.39	0.899 21.94	0.899 21.94	0.142 21.00	0.980 20.74	0.422 18.93	0.825 20.04	19.38
7036-661	B170B	0.510 21.33	0.539 20.30	0.829 18.66	0.576 21.47	0.876 21.31	0.826 21.07	0.875 21.39	0.899 21.94	0.899 21.94	0.142 21.00	0.980 20.74	0.422 18.93	0.825 20.04	19.38
7039-714	B172B	0.206 20.83	0.204 19.79	0.020 18.08	0.686 21.60	0.250 20.38	0.960 21.22	0.474 21.46	0.258 21.67	0.258 21.67	0.142 21.00	0.794 21.28	0.882 19.13	0.176 20.18	19.01
7064-656	B177B	0.909 20.49	0.871 20.19	0.211 19.09	0.973 20.63	0.316 20.40	0.240 21.37	0.863 21.20	0.302 21.46	0.302 21.46	0.142 21.00	0.871 20.76	0.255 19.74	0.487 20.34	19.50
7277-951	B246B	0.887 20.96	0.955 19.37	0.668 19.72	0.602 21.38	0.471 21.11	0.240 21.37	0.863 21.20	0.302 21.46	0.302 21.46	0.142 21.00	0.871 20.76	0.255 19.74	0.487 20.34	19.50
7278-928	B250B	0.857 20.35	0.748 19.46	0.504 18.16	0.642 21.48	0.578 21.45	0.185 21.28	0.991 20.56	0.921 21.56	0.921 21.56	0.142 21.00	0.790 20.79	0.438 19.45	0.490 20.16	19.37
7335-851	B275B	0.410 21.14	0.335 19.87	0.064 18.16	0.188 20.81	0.757 21.45	0.195 21.28	0.561 21.42	0.254 21.68	0.254 21.68	0.142 21.00	0.716 21.36	0.271 19.72	0.624 20.06	18.63
7342-791	M2016	0.834 21.02	0.501 20.41	0.111 18.39	0.221 20.95	0.514 21.12	0.393 21.76	0.626 21.33	0.682 21.86	0.682 21.86	0.142 21.00	0.193 21.40	0.513 19.21	0.670 20.16	19.41
7359-863	B282B	0.867 21.00	0.906 19.90	0.228 19.45	0.738 21.52	0.356 20.92	0.311 21.35	0.175 20.91	0.599 21.83	0.599 21.83	0.142 21.00	0.204 21.02	0.644 21.22	0.104 19.71	19.27
7366-850	B292B	0.296 20.94	0.074 19.45	0.275 19.11	0.785 <21.30	0.364 20.80	0.324 21.29	0.186 20.91	0.624 21.93	0.624 21.93	0.142 21.00	0.028 20.64	0.213 20.76	0.350 19.57	20.18
7369-844	B292B	0.811 20.98	0.668 20.61	0.446 20.29	0.477 21.38	0.896 21.37	0.806 21.93	0.973 20.60	0.738 21.93	0.738 21.93	0.142 21.00	0.028 20.64	0.213 20.76	0.350 19.57	20.18
7392-699	B300B	0.869 20.95	0.690 20.72	0.452 20.18	0.731 21.40	0.930 21.34	0.969 21.18	0.116 21.66	0.430 21.82	0.430 21.82	0.142 21.00	0.381 21.79	0.219 20.77	0.217 19.76	19.33
7417-620	B317B	0.822 20.34	0.785 20.01	0.623 20.52	0.321 21.00	0.061 20.21	0.263 21.48	0.865 21.50	0.772 21.89	0.772 21.89	0.142 21.00	0.077 20.60	0.239 21.11	0.250 19.72	20.18
7449-645	B317B	0.334 20.98	0.047 19.25	0.841 19.72	0.062 20.67	0.111 20.38	0.363 21.48	0.665 <21.38	0.059 21.32	0.059 21.32	0.142 21.00	0.022 20.59	0.307 21.14	0.286 19.88	20.08
7451-654	B327B	0.130 20.33	0.060 19.07	0.279 18.63	0.360 21.12	0.329 20.63	0.106 21.14	0.967 20.75	0.617 <21.9	0.617 <21.9	0.142 21.00	0.031 20.68	0.044 20.47	0.303 19.74	20.35
7659-954	B394B	0.192 20.60	0.085 19.37	0.286 19.26	0.402 21.36	0.055 20.35	0.096 21.36	0.242 20.85	0.011 21.71	0.011 21.71	0.142 21.00	0.599 <21.53	0.555 19.37	0.686 20.12	19.66
7660-978	B398B	0.251 20.95	0.108 19.52	0.292 19.22	0.544 21.50	0.160 20.40	0.262 21.38	0.395 21.33	0.576 <21.9	0.576 <21.9	0.142 21.00	0.906 20.67	0.591 19.73	0.957 20.54	19.17
7661-941	B402B	0.646 21.33	0.655 20.63	0.449 20.20	0.946 20.51	0.649 21.37	0.205 21.38	0.540 21.25	0.912 21.74	0.912 21.74	0.142 21.00	0.984 20.31	0.825 19.65	0.858 20.11	18.79
7684-877	B406B	0.646 21.33	0.655 20.63	0.449 20.20	0.946 20.51	0.649 21.37	0.205 21.38	0.540 21.25	0.912 21.74	0.912 21.74	0.142 21.00	0.984 20.31	0.825 19.65	0.858 20.11	18.79
7686-934	B372	0.000 20.00	0.000 20.00	0.463 <19.93	0.872 <20.74	0.872 <20.74	0.872 <20.74	0.983 20.47	0.906 21.74	0.906 21.74	0.142 21.00	0.539 21.67	0.852 20.80	0.495 19.38	20.14
7687-970	B377	0.985 20.34	0.774 20.70	0.483 20.29	0.656 21.52	0.985 20.51	0.055 21.57	0.724 21.58	0.287 21.85	0.287 21.85	0.142 21.00	0.138 21.00	0.597 19.88	0.610 20.17	19.31
7689-954	B413B	0.855 20.34	0.775 20.63	0.484 20.01	0.698 21.42	0.280 20.57	0.078 21.44	0.745 21.58	0.543 21.86	0.543 21.86	0.142 21.00	0.234 20.90	0.600 19.72	0.634 20.14	19.43
7691-882	HUBB1A	0.073 20.50	0.000 20.00	0.497 20.16	0.073 20.50	0.073 20.50	0.073 20.50	0.035 20.56	0.249 <21.6	0.249 <21.6	0.142 21.00	0.833 20.77	0.984 20.31	0.825 19.65	20.11
7713-833	H1635E	0.408 21.16	0.345 19.86	0.646 20.17	0.929 21.09	0.793 21.57	0.184 21.38	0.331 21.42	0.391 21.55	0.391 21.55	0.142 21.00	0.164 20.70	0.432 19.72	0.960 20.18	18.56
7718-874	B380	0.715 20.98	0.000 20.00	0.688 20.16	0.339 20.65	0.339 20.65	0.339 20.65	0.607 19.43	0.295 20.15	0.295 20.15	0.142 21.00	0.607 19.43	0.295 20.15	19.29	
7719-882	B386	0.000 20.00	0.000 20.00	0.688 20.16	0.449 21.0	0.449 21.0	0.449 21.0	0.642 19.64	0.562 20.18	0.562 20.18	0.142 21.00	0.642 19.64	0.562 20.18	20.15	19.08

TABLE 2—Continued

JD	Plate	V18	V20	V22	V24	V25	V26	V27	V29	V30	V34	V37	V39	V31	V42
	Phase	Phase	Phase	Phase	Phase	Phase	Phase	Phase	Phase	Phase	Phase	Phase	Phase	Phase	Phase
7721.897	8419B	0.537	20.11	0.702	19.99	0.436	21.22	0.668	21.37	0.542	21.42	0.128	21.42	0.905	19.46
7722.812	8425B	0.559	20.18	0.708	19.78	0.571	21.45	0.767	21.58	0.829	21.53	0.887	21.00	0.031	19.08
7723.729	8429B	0.643	20.52	0.813	19.52	0.719	21.52	0.875	20.86	0.929	21.53	0.887	20.31	0.131	19.61
7747.721	8389B	0.081	19.52	0.878	19.21	0.821	21.52	0.147	20.59	0.969	20.58	0.653	21.13	0.598	19.06
7748.726	8395	0.085	19.10	0.885	19.10	0.473	21.02	0.473	21.02	0.473	21.02	0.473	21.02	0.473	19.06
7752.731	8442B	0.272	19.93	0.912	18.76	0.007	21.50	0.381	20.98	0.171	21.10	0.556	21.19	0.542	19.06
7809.653	8449B	0.659	20.57	0.301	19.15	0.448	21.40	0.025	20.50	0.872	21.63	0.501	21.79	0.542	19.06
8016.953	8538B	0.570	20.62	0.717	20.42	0.189	21.22	0.700	21.31	0.301	21.56	0.618	21.71	0.706	19.44
8017.949	8544B	0.594	20.57	0.724	20.42	0.337	21.22	0.991	20.52	0.997	21.20	0.618	21.94	0.824	19.44
8018.947	8549B	0.912	20.21	0.618	20.60	0.485	21.38	0.918	20.74	0.644	21.80	0.141	20.85	0.942	19.62
8019.950	8555B	0.614	20.54	0.738	20.44	0.634	21.51	0.025	20.28	0.816	21.67	0.292	21.16	0.060	19.60
8020.951	8561B	0.665	20.53	0.745	20.41	0.782	21.53	0.134	20.43	0.988	21.03	0.442	21.38	0.178	19.67
8021.959	8559	0.689	20.63	0.752	20.40	0.932	20.63	0.593	21.51	0.243	21.63	0.297	21.31	0.297	19.67
8045.906	8566B	0.156	20.89	0.689	19.04	0.483	21.34	0.843	20.43	0.279	21.49	0.189	20.93	0.121	19.18
8046.931	8572B	0.613	21.46	0.285	19.92	0.285	21.53	0.955	20.26	0.342	21.23	0.342	21.23	0.542	19.13
8047.938	8577B	0.777	21.16	0.929	18.75	0.784	21.44	0.064	20.19	0.628	21.86	0.455	21.64	0.361	19.20
8048.942	8584B	0.321	19.92	0.936	18.77	0.933	20.53	0.173	20.54	0.801	21.75	0.644	21.47	0.479	19.63
8049.951	8588B	0.829	20.89	0.785	19.76	0.082	20.49	0.282	20.41	0.974	21.00	0.796	21.72	0.598	19.63
8050.958	8590B	0.785	20.82	0.785	19.76	0.082	20.49	0.282	20.41	0.974	21.00	0.796	21.72	0.598	19.63
8058.842	8590B	0.807	20.56	0.072	18.02	0.884	21.52	0.223	20.39	0.046	21.08	0.478	21.43	0.706	19.63
8059.826	8591B	0.830	20.66	0.072	18.02	0.884	21.52	0.223	20.39	0.046	21.08	0.478	21.43	0.706	19.63
8069.905	8592B	0.832	20.55	0.079	18.05	0.041	20.57	0.441	20.11	0.391	21.35	0.175	21.38	0.827	19.51
8070.829	8593B	0.854	20.39	0.085	18.27	0.179	21.08	0.441	20.11	0.391	21.35	0.175	21.38	0.827	19.51
8071.830	8597B	0.191	20.95	0.878	18.60	0.327	21.20	0.558	21.13	0.564	21.72	0.621	21.91	0.061	19.53
8071.909	8598B	0.195	20.84	0.093	18.50	0.339	21.20	0.658	21.33	0.736	21.84	0.081	20.72	0.179	19.66
8072.826	8599B	0.251	21.02	0.099	18.37	0.475	21.52	0.667	21.41	0.750	21.72	0.093	20.82	0.188	19.71
8072.903	8600B	0.256	21.16	0.100	18.54	0.486	21.52	0.774	21.33	0.920	21.53	0.242	21.09	0.306	19.51
8073.821	8601B	0.904	20.30	0.106	18.62	0.622	21.52	0.874	20.96	0.078	21.08	0.380	21.31	0.414	19.51
8074.911	8603B	0.312	21.17	0.925	19.86	0.784	21.52	0.993	20.10	0.420	21.46	0.543	21.59	0.542	19.66
8075.806	8604B	0.432	21.20	0.951	19.25	0.917	20.91	0.993	20.10	0.420	21.46	0.543	21.59	0.542	19.66
8075.880	8605B	0.975	19.17	0.120	18.47	0.928	20.64	0.098	20.29	0.432	21.56	0.689	21.74	0.657	19.50
8077.809	8606B	0.000	19.20	0.000	18.50	0.000	19.20	0.000	19.20	0.000	19.20	0.000	19.20	0.000	19.50
8078.802	8607B	0.044	19.20	0.140	18.75	0.361	21.25	0.415	20.71	0.935	21.62	0.128	20.84	0.001	19.50
8079.812	8612B	0.068	19.72	0.154	18.54	0.211	21.52	0.525	21.16	0.109	21.22	0.280	21.08	0.121	19.18
8080.816	8615B	0.147	20.58	0.193	18.47	0.091	21.48	0.634	21.57	0.281	21.56	0.430	21.55	0.239	19.47
8366.955	8690B	0.147	20.58	0.193	18.47	0.091	21.48	0.634	21.57	0.281	21.56	0.430	21.55	0.239	19.47
8367.935	8694B	0.936	19.45	0.115	19.08	0.236	20.51	0.697	21.59	0.478	21.55	0.391	21.29	0.389	19.66
8406.943	8703B	0.580	21.39	0.382	19.53	0.021	20.57	0.805	20.23	0.394	21.50	0.215	21.84	0.704	19.71
8430.877	8737B	0.037	20.30	0.546	20.19	0.571	21.52	0.533	21.32	0.350	21.50	0.386	21.93	0.528	19.71
8431.872	8719B	0.460	19.97	0.553	20.37	0.718	21.52	0.633	21.32	0.350	21.50	0.386	21.93	0.528	19.71
8482.764	8721B	0.673	20.65	0.901	18.79	0.264	21.00	0.745	20.47	0.390	21.53	0.007	21.18	0.648	19.63
8483.751	8728B	0.697	20.41	0.907	18.53	0.552	21.49	0.480	21.27	0.480	21.27	0.069	20.67	0.548	19.63
8484.701	8730B	0.719	20.65	0.914	18.64	0.552	21.49	0.480	21.27	0.480	21.27	0.069	20.67	0.548	19.63
8485.727	8732B	0.744	20.70	0.920	18.43	0.705	21.52	0.592	21.35	0.592	21.35	0.040	21.48	0.876	19.57
8779.931	HL880H	0.375	20.85	0.931	18.65	0.332	21.52	0.532	20.90	0.483	21.52	0.395	21.53	0.997	19.57
8780.974	8811B	0.338	21.04	0.938	18.07	0.486	21.40	0.645	21.29	0.552	21.53	0.552	21.53	0.821	19.57
8781.920	8815B	0.396	20.98	0.944	18.03	0.657	21.47	0.748	20.55	0.825	21.73	0.694	21.55	0.933	19.57
8782.920	8819B	0.457	20.48	0.951	17.99	0.775	21.52	0.867	21.09	0.997	20.26	0.844	21.70	0.051	19.57
8783.933	8823B	0.476	20.45	0.951	17.99	0.775	21.52	0.867	21.09	0.997	20.26	0.844	21.70	0.051	19.57
8784.933	8827B	0.476	20.45	0.951	17.99	0.775	21.52	0.867	21.09	0.997	20.26	0.844	21.70	0.051	19.57
8785.933	8831B	0.476	20.45	0.951	17.99	0.775	21.52	0.867	21.09	0.997	20.26	0.844	21.70	0.051	19.57
8786.933	8835B	0.476	20.45	0.951	17.99	0.775	21.52	0.867	21.09	0.997	20.26	0.844	21.70	0.051	19.57
8786.909	8836B	0.639	21.26	0.923	17.56	0.367	20.82	0.180	20.49	0.512	21.72	0.144	20.81	0.286	19.03
8787.873	8841B	0.758	20.93	0.985	17.68	0.509	21.38	0.443	21.81	0.915	21.29	0.463	21.46	0.321	18.78

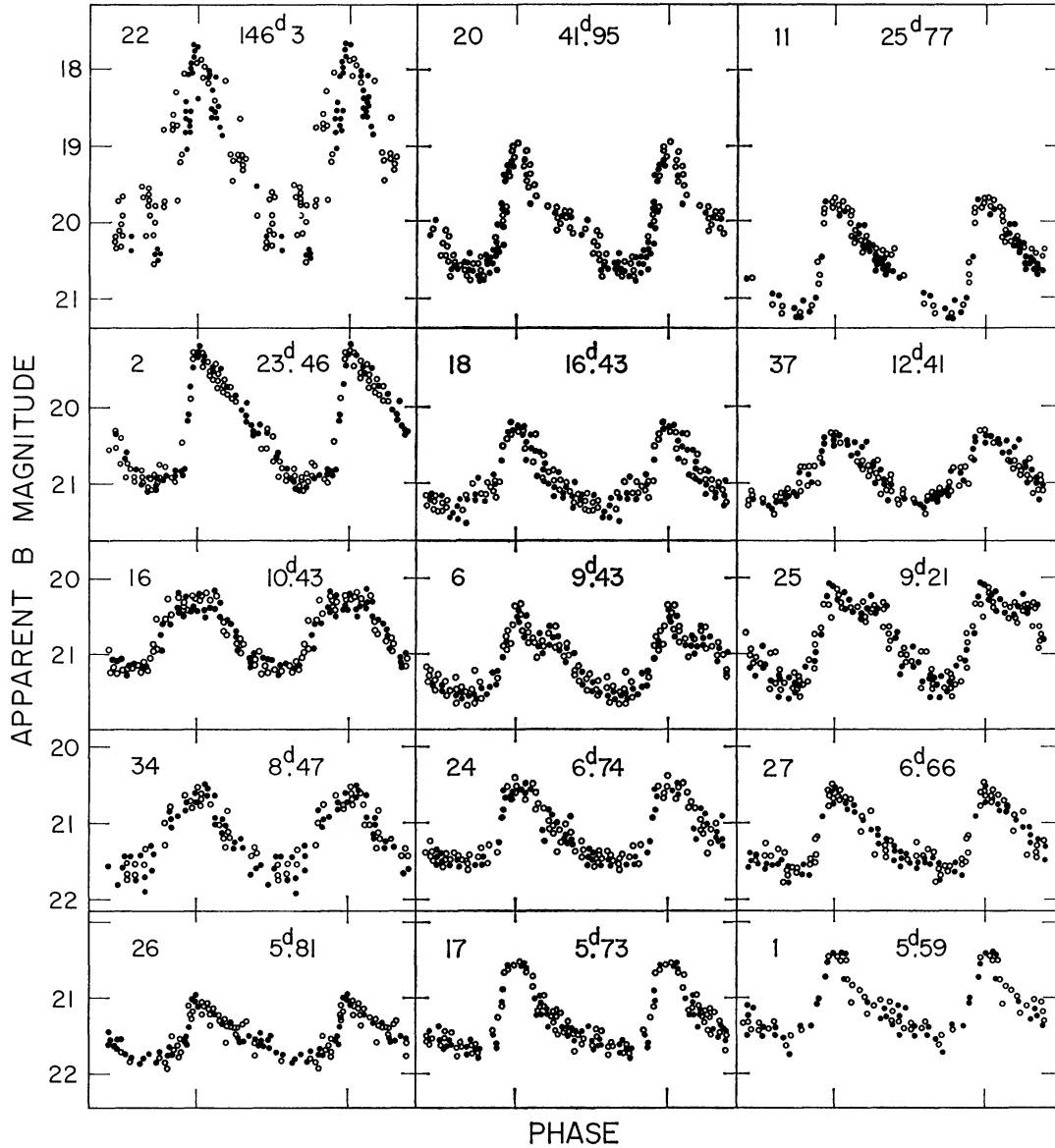


FIG. 7—Blue light curves for Cepheids arranged in order of period. Data are from Table 2.

period known. That the star is undoubtedly a Cepheid follows from the shape of the light curve and from classification of a spectrum taken by Baade with the 100-inch (14 hours exposure) during a maximum in 1941 September ($m_{pg} = 17.5$). Baade comments on the spectrum: "Joy classified the type as cK2 by the following arguments, (1) Ca I $\lambda 226$ is strong. This line does not occur [in such strength] earlier than K0. (2) [The high luminosity lines of] Sr II $\lambda 215$, $\lambda 4077$ are present. (3) Joy states that H and K are somewhat sharper than expected, which is consistent with the high luminosity. Humason classified the spectrum as F5 to G0 from the strength of the hydrogen lines and the H and K lines only. His early spectral type is consistent with Joy's later type since it is well known that hydrogen lines have abnormal strength in Cepheids of Type I. Adams and Joy (1918) stated many years ago that at maximum light the spectral class

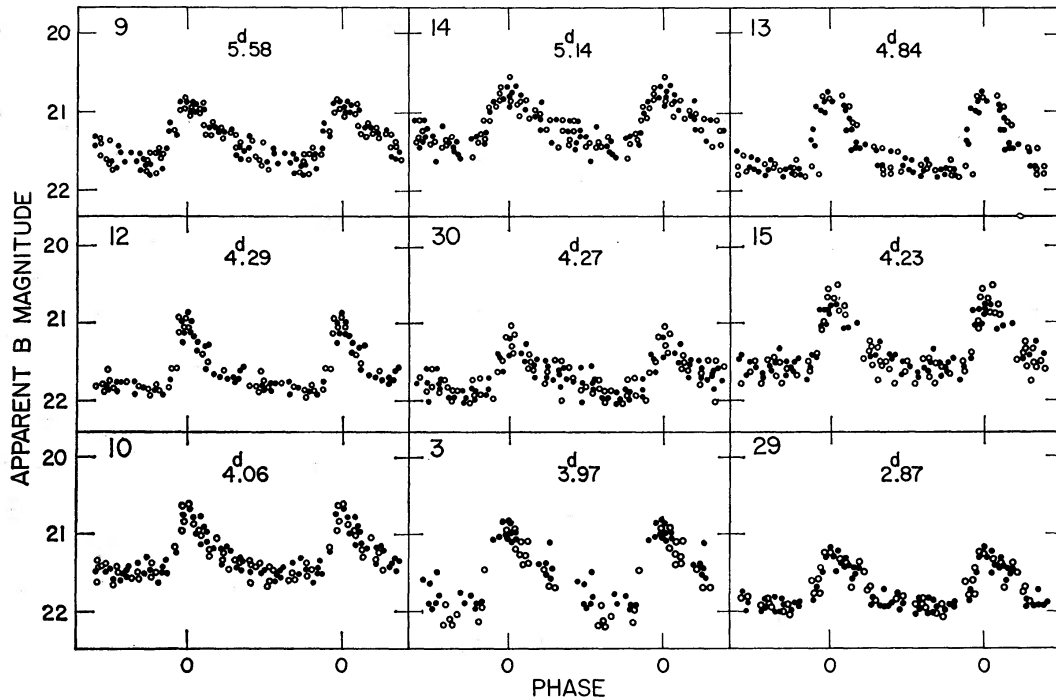


FIG. 8.—Same as Fig. 7 for the remaining Cepheids

of a Cepheid is on the average 8 spectral subdivisions earlier when classified from hydrogen lines than from general metal lines." This description shows that the spectrum of V22 is similar to that of other Cepheids of shorter period, and that there should be no hesitation in assigning it to the Cepheid class.

The only other abnormal variable is V39, which Baade did not classify as a Cepheid for two reasons: (a) The shape of the light curve is quite unusual, as shown in Figure 9. The rise to maximum and fall to a first minimum is symmetrical about the phase ± 0.2 . Centered at phase 0.5 is a second lower maximum. The light curve can be described as an *inverted* β Lyrae eclipsing variable, and appears to be unique among Cepheids. Because of the peculiar light curve, various attempts have been made to disprove the period. Harold Weaver, working with Baade on other problems sometime after 1940, obtained a period of 28^d687 after many trials at other periods. Baade himself obtained $P = 28^d71$ from the material from 1932 to 1937. G. A. Tammann recently reworked the problem and obtained what is here adopted as $P = 28^d720$. There appears to be no

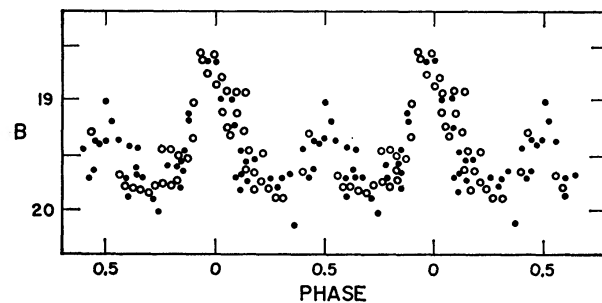


FIG. 9.—Light curve for the peculiar regular variable V39. The star is considered to be a Cepheid in the text, but was not so considered by Baade. It lies high in the P-L relation.

possibility that this period is spurious because of the dense distribution of plates, especially in 1935. (b) Baade's second reason was that V39 falls 0.9 mag brighter than the apparent P-L relation for the twenty-four other Cepheids. Baade's interpretation was that the P-L relation has only a very small intrinsic scatter about the ridge line ($\sigma \simeq 0.15$ mag), and because V39 differed by 6σ from this line the variable was not considered to be a Cepheid, despite the high regularity of its period and light curve. A new interpretation of the data is discussed in § IV.

The only other point to be mentioned concerns the Hertzsprung (1926) relation between light-curve shapes and period. Hertzsprung first noticed that if light curves of Cepheids are ordered by period, a systematic perturbation occurs on an otherwise smooth curve in the period interval from 6 to 16 days. At the short-period limit, a hump appears on the descending part of the curve, just prior to minimum light. The hump progressively moves toward the maximum as the period increases, producing double maxima near 9 days, then a single-peaked maximum near 10 days, moving through the maximum phase to appear on the ascending branch for periods between 10 and 16 days. For longer-period stars such as RU Sct ($P = 19^d70$), SW Vel ($P = 23^d47$), X Pup ($P = 25^d96$), and U Cen ($P = 38^d76$) the hump again appears on the descending branch but with less prominence than for stars with periods between 6 and 9 days. The phenomenon is general, occurring among Cepheids in M31 (cf., e.g., Baade and Swope 1963, 1965), the SMC (cf. Gaposchkin and Gaposchkin 1966), and the LMC (Mohr 1938). A convincing theoretical explanation has been given by Christy (1970) in terms of a reflection by the core of accelerations originating in the helium-ionization zone. The reflected pulse, upon reaching the surface after traveling entirely through the star, appears at various phases in the light curve depending on the travel time.

The Hertzsprung phenomenon appears only weakly in Figures 7 and 8, principally because the critical period range is not well represented. However, the double maximum near 9 days is clearly visible in V25 ($P = 9^d21$) and V6 ($P = 9^d43$), with some indication of a perturbation near maximum for V34 ($P = 8^d47$) and V16 ($P = 10^d43$), and a moderately definite indication of a hump on the ascending branch for V37 ($P = 12^d41$) and V18 ($P = 16^d43$).

The final remarks on Figures 7 and 8 concern the limiting magnitude of the 100-inch telescope during these prewar years when the Los Angeles valley was relatively dark. The working limit appears to be $B \simeq 22.2$ as shown for V3 of Figure 8. The actual limit for detectability was somewhat fainter, perhaps at $B = 22.5$. We earlier determined that the limit of the Mount Wilson 60-inch was $B \simeq 21.5$ before 1950 (Tammann and Sandage 1968), which is in essential agreement with $B \simeq 22.5$ for the 100-inch, when one considers the ratio of the apertures, at the same focal ratio of $f/5$ for both telescopes.

e) Irregular Variables

Eleven irregular variables are listed in Table 1. Of these, eight are very red and are undoubtedly similar to those found in the h and χ Per association. Similar red variables are found in M31 (Baade and Swope 1963, 1965), M33 (Humason and Sandage, unpublished), NGC 6822 (Kayser 1967), and NGC 2403 (Tammann and Sandage 1968). Of the other three variables, V21 and V42 are of intermediate color and V44 is very blue, perhaps of the type discussed by Hubble and Sandage (1953) in M31 and M33, but much fainter intrinsically.

The final column of Table 2 lists B magnitudes for the unusual irregular V42. Table 3 lists individual magnitudes from 1929 to 1942 for V23, V32, V43, V44, V45, and V56. These, together with V52 (which was seen only in the 1935–1936 season, rising above plate limit to $B = 21.5$), are illustrated in Figure 10. Variations on a scale of 100 days are evident for the red stars, and the longer-term variation on a scale of several years characterizes the blue irregular V44.

TABLE 3
B MAGNITUDES OF NON-CEPHEIDS

JD 2,420,000 +	V23	V32	V43	V44	V45	V56
5830	19.99	19.13	19.44	20.58	19.70	19.40
6212	20.05	19.02	20.68	19.75	19.28
6269	19.83	19.35	19.44	20.77	19.77	19.28
6306	19.99	19.51	20.68	19.76	19.28
6595	19.72	19.71	19.17
6620	20.14	19.60	19.86	20.65	19.93	19.12
6689	19.77	19.40
6925	20.14	19.53	19.71	20.54	19.94	19.37
6956	19.51	19.75
6958	19.61	19.30
6960	20.29	19.74	20.61	20.25
6988	20.56	19.77	19.68	20.68	19.89	19.28
7010	20.80	19.79	19.60	20.68	20.13	19.37
7040	20.84	19.80	19.70	20.62	20.08	19.28
7066	20.85	19.80	20.73	19.92	19.48
7278	20.10	19.01	20.73	19.77	19.10
7312	20.08	19.14	19.45	20.62	19.77	19.14
7340	20.08	19.52	19.26	20.73	19.94	19.28
7360	20.10	19.68	19.18	20.66	19.93	19.38
7395	20.38	19.74	19.65	20.65	19.80	19.40
7418	20.43	19.77	19.70	20.56	19.77	19.40
7450	20.45	19.77	19.99	20.51	19.77	19.40
7662	20.21	19.81	19.81	20.11	20.13	18.90
7688	19.77	19.58	20.12	19.38
7690	20.04	20.11	19.25
7692	19.91	19.67	20.08
7720	19.77	19.86	19.88	19.18
7725	20.01	19.85	20.09
7750	20.04	19.85	19.83	20.03	19.85	19.30
7790	20.09
7810	20.47	19.73	19.71	19.80	19.45
8020	20.04	19.50	19.77	20.01	20.20	19.50
8049	20.00	19.61	19.83	19.98	20.20	19.68
8073	19.92	19.63	19.84	20.02	20.34	19.60
8370	20.13	19.91	19.77	20.04	19.61	19.40
8408	20.47	19.94	19.94
8432	20.38	19.99	19.73	20.06	19.65	19.70
8485	20.05	20.05	19.71	20.08	19.84	19.45
8516
8783	20.45	19.99	19.74	20.24	19.84	19.32
9200	20.01	19.77	19.74	20.32	20.41
9530	20.28	19.62	19.76	20.33	19.80
9550	20.01
9850	20.43
9880	20.70
9900	20.16
9920	20.11
9980	19.98
30320	20.32

Four stars not illustrated have the following characteristics:

V21.—Intermediate color and small amplitude. From 1929 to 1937 the star varied from $B = 19.60$ to $B = 20.34$. The largest variations occurred between 1929 and 1932, after which the star remained relatively constant to within ± 0.2 mag at $B \simeq 20.0$.

V38.—Very red. Optical double. The variable is the eastern component. From 1933 to 1937 the star was very nearly constant at $B = 19.2$. The greatest variability occurred in 1931 and 1932, when the star reached $B = 18.6$ in one burst in 1932, and with less certainty $B \simeq 18.5$ in 1931. At faintest minimum, the star was $B = 19.6$, which occurred in 1933. This star is one of the brightest red variables in the galaxy, reaching $M_B = -6.0$ at maximum (or $M_V \simeq -8.0$ if a color of 2.0 is assumed).

V42.—Intermediate color. Rapid changes of 0.6 mag in intervals of 3 days. Especially rapid changes of this type were observed in 1934, 1935, and 1937. The star was considered to be possibly periodic ($P \simeq 80^{\text{d}}$), but no satisfactory analysis has been achieved. It is one of the brightest stars in the galaxy at maximum light ($B \simeq 18.5$, $M_B = -6.0$).

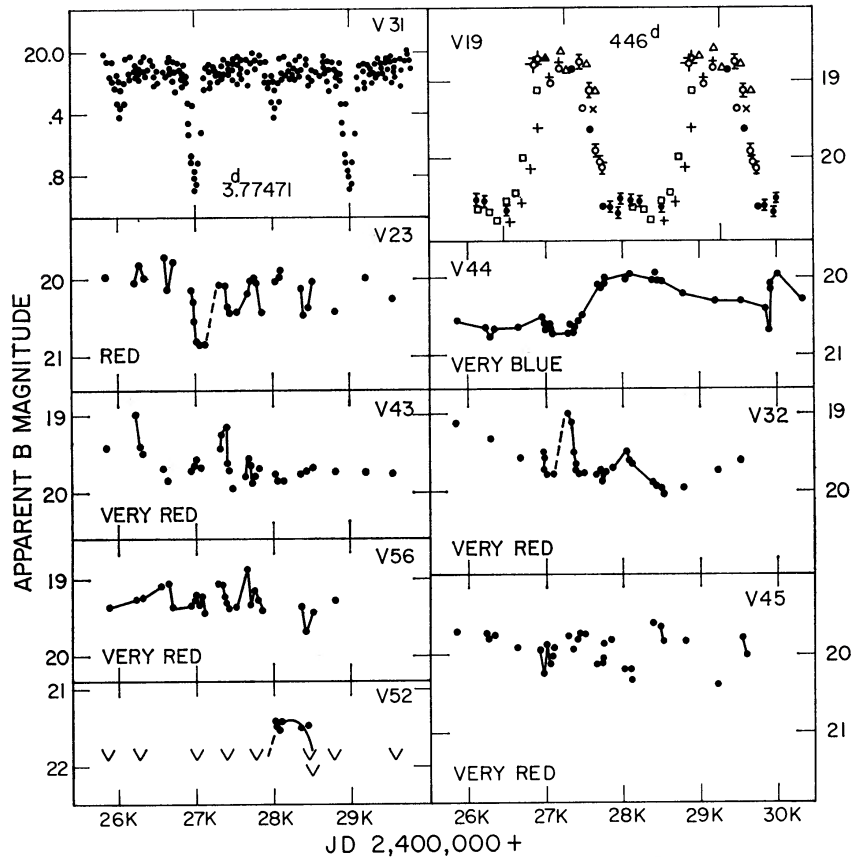


FIG. 10.—Light curves for seven irregular variables, for the eclipsing binary, and for the semiregular red star V19. Data are from Tables 3 and 5. Only data from 1929 to 1937 are plotted for V19, where the symbols \times , \bullet , \circ , $+$, \square , \ominus , \triangle , and \diamond are used in succession for the nine years.

V50.—Reddish color but not extreme. Slow variation of small amplitude, ranging from $B = 20.45$ to $B = 20.93$ in a sinusoidal fashion from 1930 to 1937. Its “period” is ~ 2600 days.

Table 4 summarizes the characteristics of the irregular variables. The final column lists absolute magnitudes at maximum light, if an apparent blue modulus of $(m - M)_{AB} = 24.55$ (§ IV) is assumed.

f) The Semiregular Variable V19

The light curve for V19 is shown in Figure 10 as plotted from the data listed in Table 5. The variable presents problems in classification. The period is moderately regular, as shown by the well-defined light curve plotted from 11 cycles covered between 1929 and 1946. The light curve does not repeat perfectly from cycle to cycle, but the period appears to be relatively stable. For example, the star rose toward maximum more rapidly and fell toward minimum more slowly during the 1939–1940 season than in other cycles, artificially giving the appearance of a flat top to Figure 10.

The amplitude of only $A_B = 2.2$ mag is too small for a normal Mira according to the standard definition (cf. Kukarkin *et al.* 1957), but the period may be too regular for the object to be classed as a semiregular variable. We are forced, however, to an SRC classification because of the absolute magnitude. If V19 is in IC 1613, its absolute magnitude at maximum is $M_B \simeq -6.0$, which is far brighter than any Mira (Merrill and Wilson

TABLE 4
SUMMARY OF IRR VARIABLES

No.	B(max)	B(min)	A_B	Color	M_B (max)
21.....	19.60	20.34	0.74	INT	-4.95
23.....	19.72	20.85	1.13	R	-4.83
32.....	19.00	20.05	1.05	VR	-5.55
38.....	18.6	19.6	1.0	VR	-5.95
42.....	18.5	19.8	1.3	I	-6.05
43.....	19.02	19.99	0.97	VR	-5.53
44.....	20.00	20.78	0.78	VB	-4.55
45.....	19.60	20.40	0.80	VR	-4.95
50.....	20.45	20.93	0.48	I-R	-4.10
52.....	21.4	>22	>0.8	?	-3.15
56.....	18.90	19.70	0.80	VR	-5.65

TABLE 5
PHOTOMETRY OF THE SEMI-REGULAR V19

JD 2,400,000+	E	Phase	B	JD 2,400,000	E	Phase	B	JD 2,400,000	E	Phase	B
25,830	-3	0.175	19.38	27,661	1	0.280	20.65	29,194	4	0.718	18.65
26,212	-2	0.031	18.87	685	1	0.334	20.73	197	4	0.725	18.63
269	-2	0.159	19.65	691	1	0.348	20.54	552	5	0.520	19.98
305	-2	0.240	20.65	721	1	0.415	20.57	612	5	0.656	18.87
595	-2	0.890	19.05	749	1	0.478	20.57	848	6	0.185	18.60
620	-2	0.946	18.84	810	1	0.614	20.65	871	6	0.235	18.89
689	-1	0.101	19.37	28,019	2	0.083	18.76	903	6	0.308	19.61
927	-1	0.635	20.83	048	2	0.148	19.13	933	6	0.376	19.96
959	-1	0.706	20.58	071	2	0.199	19.93	969	6	0.455	20.01
986	-1	0.767	20.15	075	2	0.208	20.07	30,226	7	0.031	18.54
27,009	-1	0.818	19.63	080	2	0.220	20.12	236	7	0.054	18.09
039	-1	0.886	18.98	367	2	0.863	18.70	259	7	0.105	18.49
065	-1	0.944	18.79	407	2	0.953	18.58	322	7	0.246	19.05
278	0	0.422	20.66	432	3	0.009	18.85	613	7	0.899	18.26
312	0	0.498	20.69	484	3	0.126	18.77	641	7	0.962	18.22
339	0	0.558	20.81	516	3	0.197	19.13	672	8	0.031	18.37
365	0	0.617	20.58	782	3	0.794	18.80	705	8	0.105	18.68
393	0	0.679	20.47	786	3	0.803	18.73	727	8	0.155	18.39
418	0	0.735	20.00	787	3	0.805	18.47	32,031	11	0.078	18.47
451	0	0.809	19.15	193	4	0.715	18.74				

Phase computed from Max at JD 2427090 + 446^d.n

1942; Osvalds and Risley 1961; Smak 1966). That it is not a foreground Mira or an ordinary giant SRa or SRb ($M_V \simeq -1$) follows from its faintness at $B(\text{max}) = 18.6$, which would place it at intergalactic distances (i.e., $m - M \simeq 19.6$). We therefore believe that V19 belongs to IC 1613, and that the best classification is an abnormally regular example of the supergiant SRC class whose members include μ Cep, α Ori, α Sco, and RW Cyg, all of which are of exceeding high luminosity (usually luminosity class Ia).

g) *The Eclipsing Variable and a Nova*

Figure 10 shows the light curve for V31, which is a typical eclipsing binary of the Algol type with a definite secondary minimum at phase 0.5. The star is very blue, and has a period of 3^d.77. The magnitudes are $B = 20.15$ at maximum, 20.90 at primary minimum, and 20.42 at secondary minimum.

One nova was found by Baade with the 200-inch in 1954 November. The position is marked in Figures 1 and 2. The nova had an extremely rapid rise. It was invisible on a

200-inch plate taken 1954 November 21, but was present on three plates taken 24 hours later at $B \simeq 17.5$. No further plates of IC 1613 were taken during that season, and the star was not seen again. With $(m - M)_{AB} = 24.55$, the absolute magnitude was $M_B = -7.0$ on November 21. Very likely the nova was caught before its maximum.

IV. PERIOD-LUMINOSITY RELATION AND THE DISTANCE

Table 6 lists elements for the twenty-five Cepheids shown in Figures 7, 8, and 9. The periods in column (3) are as derived by Baade. Column (4) gives the error of these periods (in units of 10^{-5} days) derived by finding the limits of period change which would cause detectable phase spreading in the plotted light curves. The intensity mean $\langle B \rangle$ in the penultimate column was found by converting the light curves to intensity units, planimetry, and converting back to magnitudes. The P-L relation can be discussed from these data.

a) Baade's Interpretation

Figure 11 shows the P-L relation without V39, as plotted from the data in Table 6. A least-squares line gives $\langle B \rangle = -1.518 \log P + 22.422$ which is shown as the heavy ridge line in Figure 11. The scatter from this line, read as a magnitude residual, gives $\sigma(M) = 0.158$ mag. The two boundary lines in the diagram are drawn at $\pm 2 \sigma = \pm 0.32$ mag. For a normal distribution, 95 percent of the sample should be enclosed within these boundaries, and this is the case.

Two points concerning this solution are very disturbing: (1) the slope of the P-L relation is exceedingly small compared with the relation in other galaxies; (2) the dispersion is smaller by a factor of 2 than is required by available data on the width of the instability strip for Cepheids in the H-R diagram for all other galaxies in the Local Group. Both points are serious, as shown by the following preponderance of evidence to the contrary.

TABLE 6
ELEMENTS OF 25 CEPHEIDS AND ONE ECLIPSER IN IC 1613

No	JD 2,420,000+	P(days)	$E^d \times 10^5$	log P	B(MAX)	B(MIN)	B(MED)	$\langle B \rangle$	A_B
1	7,931.28	5 ^d 59210	#28	0.748	20.45	21.55	21.00	21.12	1.14
2	7,391.11	23.4611	170	1.370	19.20	20.98	20.09	20.30	1.78
3	8,049.88	3.96789	21	0.599	20.94	22.00	21.47	21.61	1.06
6	7,718.77	9.43048	19	0.974	20.40	21.56	20.98	21.04	1.16
9	8,073.59	5.57738	37	0.746	20.94	21.66	21.30	21.37	0.72
10	7,723.80	4.06529	16	0.609	20.60	21.50	21.05	21.31	0.90
11	7,807.01	25.7719	250	1.411	19.74	21.20	20.47	20.47	1.46
12	7,689.83	4.28604	22	0.632	20.92	21.86	21.39	21.63	0.94
13	8,017.00	4.84448	10	0.685	20.76	21.78	21.27	21.37	1.02
14	8,016.97	5.14450	18	0.711	20.70	21.48	21.09	21.15	0.78
15	7,311.963	4.22744	13	0.626	20.66	21.60	21.13	21.33	0.94
16	7,370.03	10.43584	39	1.019	20.26	21.20	20.73	20.66	0.94
17	8,067.631	5.73687	18	0.759	20.56	21.66	21.11	21.21	1.10
18	7,361.98	16.4353	200	1.216	20.26	21.32	20.79	20.89	1.06
20	7,279.84	41.953	500	1.622	18.98	20.64	19.81	19.86	1.66
22	8,058.3	146.35	23000	2.166	17.74	20.40	19.07	19.07	2.66
24	7,752.68	6.74350	19	0.829	20.53	21.50	21.01	21.08	0.97
25	7,393.358	9.2112	20	0.960	20.10	21.44	20.77	20.67	1.34
26	7,689.50	5.81614	7	0.765	20.98	21.84	21.41	21.49	0.86
27	8,044.65	6.66043	48	0.820	20.56	21.62	21.09	21.16	1.06
29	8,017.957	2.869059	2	0.458	21.21	21.94	21.58	21.76	0.73
30	7,660.93	4.26963	22	0.630	21.10	21.90	21.50	21.64	0.80
34	8,078.796	8.47833	4	0.928	20.52	21.60	21.06	21.12	1.08
37	7,662.14	12.4140	330	1.084	20.38	21.31	20.85	20.87	0.93
39	6,926.00	28.720	1.458	1.458	18.60	19.90	19.25	1.30
31	8,049.935	3.77471	4	0.577	20.10	20.90	0.80

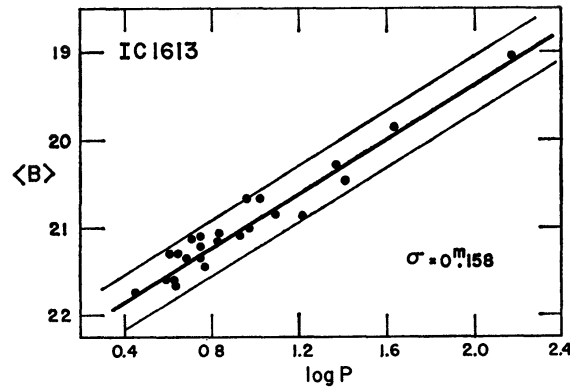


FIG. 11.—Baade's interpretation of the P-L relation from data in Table 6. Variable 39 is excluded, and the bias caused by the absence of known Cepheids that disappear below plate limit at minimum is neglected. Least-squares equation of the ridge line is $B = -1.518 \log P + 22.42$.

1. The slope of the P-L relation is well determined to be near -3.00 in the Magellanic Clouds. The data of Woolley *et al.* (1962) gave $d\langle B \rangle / d \log P = -2.85$. The result was confirmed by Gascoigne and Kron (1965), and more recently by Gascoigne (1969).⁴ Arguments were presented by Sandage and Tammann (1968, Figs. 1 and 4) that the slope of the P-L relation for Cepheids in LMC, SMC, M31, and NGC 6822 is the same, and that in the linear part of the P-L relation its value is close to $d\langle B \rangle / d \log P = -2.85$. In view of these extensive data, the very small slope of -1.5 for IC 1613 in Figure 11 would be most disturbing because it would be the first evidence for a significant difference in the intrinsic properties of Cepheids in different galaxies.

2. The intrinsic width of the P-L relation is a result of the finite width of the instability strip in the H-R diagram (Sandage 1958). The available data from our own and other galaxies shows that the composite P-L relation has a rather well-defined intrinsic width of $\Delta B = \pm 0.60$ mag (Sandage and Tammann 1968) for members of the Local Group. This requires (cf. eq. [5] of Sandage and Tammann 1968) that the total width of the H-R strip be $\Delta(B - V) = \Delta M_B / 3.52 = 0.34$ mag, which is close to what is observed (cf. Dickens and Carey 1967, Fig. 8; Christy 1970, Fig. 11). But the intrinsic spread of the P-L relation for IC 1613 is only $\pm 2 \sigma = \pm 0.32$ mag, which is anomalously small by a factor of 2.

If these differences between IC 1613 and other galaxies are real, then the base upon which distance determinations to galaxies are made becomes suspect, because if differences exist among Cepheids, they may exist among other indicators (brightest stars and sizes of H II regions). However, an alternative explanation of Figure 11 appears possible.

b) Alternative Interpretation and the Distance

Figure 12 shows the data of Figure 11 and Table 6, together with the added variable V39 (Fig. 9). Superposed are the boundary lines of the P-L relation previously established from other galaxies of the Local Group (Sandage and Tammann 1968, Table A1) as later revised by 0.05 mag (Sandage and Tammann 1969). The upper panel shows the data at maximum light; the lower, at mean light. The fit has been made so that no stars exist outside the boundary lines in $\langle B \rangle$, and equal deviations exist above and below the lines in $B(\max)$.

Known observational selection effects explain at least part of the nonuniform filling

⁴ The earlier contrary result of Arp (1960) in the SMC that $d\langle B \rangle / d \log P \simeq -2.25$ is discussed by Gascoigne and Kron (1965), by Gascoigne (1969), and by Andrews working at Pretoria, and is attributed to a scale error in Arp's magnitudes fainter than $V \simeq 14$.

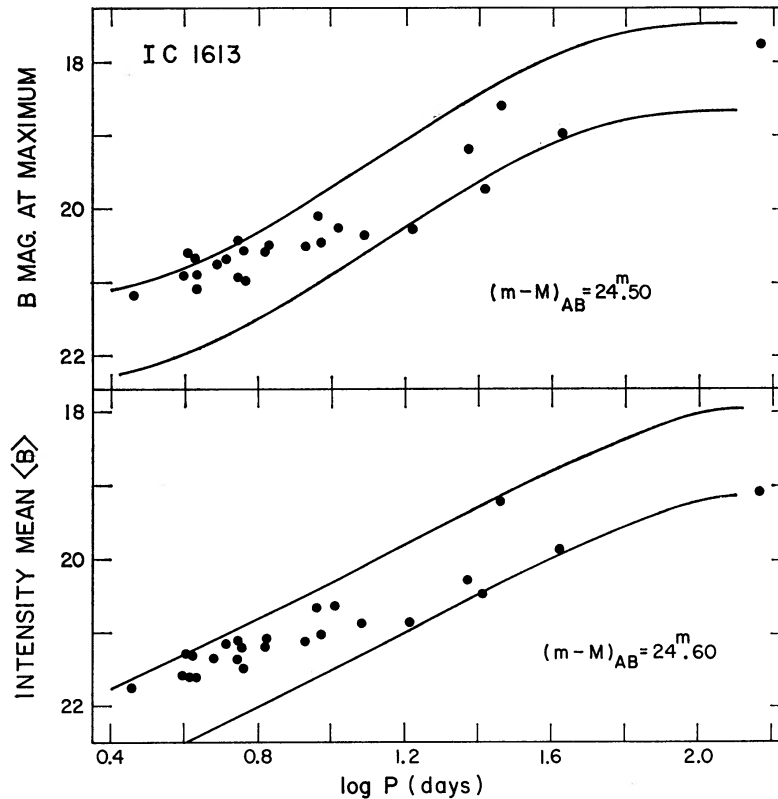


FIG. 12.—Preferred interpretation of the P-L relation. Boundary lines are from the calibration of Sandage and Tammann (1968) as derived from galaxies in the Local Group and later modified by 0.05 mag brighter (Sandage and Tammann 1969).

of the boundaries in Figure 12. (1) Baade studied only those variables which were above plate limit at all phases. Many fainter variables are known in the period interval from 2 to 9 days (V7, 28, 35, 36, 47, 48, 49, 53, 54, 59, 60, 61, and 62; see Table 1). When the light curves are eventually obtained, these stars will appear in the fainter regions of Figure 12 in the interval $0.95 \geq \log P \geq 0.3$. (2) It is known (Sandage and Tammann 1971) that Cepheids in this period range have maximum amplitudes at the blue edge of the instability strip, monotonically decreasing toward the red. By a well-known argument, the blue edge of the strip maps into the upper envelope line of Figure 12; the red edge, into the lower. Hence, the probability of discovery of the faintest Cepheids decreases as one proceeds from left to right in Figure 12 near $\langle B \rangle \simeq 21.8$, and this adds to the bias.

Although reasonable at the faint end, these two effects do not explain the lack of bright stars near the upper envelope for $\log P > 1.2$ in Figure 12. However, the number of stars is so small that small-sample statistics may be involved. An important test of the correctness of the fitting procedure in Figure 12 would be to correlate colors with magnitude deviations from the P-L ridge line. Comparison with the well-defined correlations which exist for Cepheids in the LMC, the SMC, and the Galaxy (Sandage and Tammann 1968, 1969) should be decisive for a choice between the fit of Figure 11 and the fit of Figure 12. Colors are not now available, and the problem remains to be investigated.

The present decision has been to accept Figure 12 as more reasonable than Figure 11, and to adopt the mean apparent blue modulus as $(m - M)_{AB} = 24.55$. The reddening is $E(B - V) = 0.03$ mag (Sandage 1962, Table 1; and the Appendix here), giving $(m - M)_0 = 24.43$ as the true modulus. The total integrated luminosity is then $M_B \simeq$

−14.45 which follows from Holmberg's (1950) measurement of $m_{pg}(\text{total}) = 10.00$ which transforms to $B = 10.10$.

V. BRIGHTEST BLUE AND RED STARS

The absolute magnitude of the brightest stars in galaxies is a function of integrated galaxian luminosity. The data in IC 1613 are important in calibrating this relation at the faint end (Sandage and Tammann 1971).

The brightest star that can definitely be assigned to IC 1613 is the comparison star 22A, marked on the NE₂ identification chart of Figure 3 (Plate 3). The star is extremely blue, and is undoubtedly a member of the galaxy. The magnitude and color, listed in Table A2 of the Appendix, are $B = 17.00$, $B - V = -0.15$. Using the apparent modulus of $(m - M)_{AB} = 24.55$ gives $M_B = -7.55$. This is considerably fainter than the brightest stars of more luminous galaxies, such as M33 where the brightest blue stars reach $M_B \simeq -9.5$, or M101 where they are brighter than $M_B \simeq -10.0$. Star 22A is near the center of an ill-defined H II region later marked as number 19. The star occurs with several other bright blue stars and with the longest-period Cepheid (V22). These form a small association of about 15'' in diameter (52 pc at a true modulus of $(m - M)_0 = 24.43$). A more prominent association containing stars which are almost as bright is centered on the well-developed H II region later called number 10 (§ VI). This association is also about 50 pc in diameter.

The brightest red stars have been found by blinking a matched pair of 200-inch 103a-O and 103a-D plates. Many of these are variable, and the brightest of these are listed in Table 4. The variable V42 at $B(\text{max}) = 18.5$ is followed closely in brightness by V38 with $B(\text{max}) = 18.6$, V56 with $B(\text{max}) = 18.9$, and V43 with $B(\text{max}) = 19.0$, corresponding to absolute magnitudes M_B between −6.05 and −5.53. Visual magnitudes have not yet been measured, but provisional colors of $B - V \simeq +2.0$ put $M_V = -8.05$ for the absolute magnitude of the brightest red supergiants. This agrees well with M_V values for the brightest red stars in other galaxies (Tammann and Sandage 1968). Curiously, the brightest luminosity for red supergiants appears to be independent of total luminosity of the parent galaxy, in contrast to the situation for brightest blue stars. A more complete discussion is given elsewhere (Sandage and Tammann 1971).

VI. LINEAR SIZES OF THE H II REGIONS

Nineteen H II regions are marked in Figure 13 (Plate 7), which is from a 200-inch plate taken by Baade on Eastman 103a-E + RG1 filter. IC 1613 has very few H II regions; and of the nineteen marked, all but three are concentrated in the northeast sector of the galaxy. Most have low surface brightness, although numbers 8, 11, and 19 are exceptions. These are small. Number 8 has a major diameter of 5".4 ($d = 20$ pc), while number 11 is only 2'' in diameter ($d = 7$ pc). The radial velocity of the galaxy was determined by Humason from spectra of number 8.

The intricate pattern of overlapping regions in the northeast quadrant is shown in the enlargement of Figure 14 (Plate 8). Region 10 appears as a classical Strömgren sphere which contains several of the brightest blue stars in the galaxy near its center.

Only regions 10, 3, 14, and the ring region number 1 are well enough defined among the larger regions to give useful angular diameters. The linear dimensions, are: $d = 44".6$ (167 pc) for number 10; $d = 34".0$ (127 pc) for number 3; $d = 19".4$ (72 pc) for 14, and $d = 15".7$ (59 pc) for number 1 according to the measurements by Baade. These dimensions are much smaller than the largest H II regions in brighter galaxies such as NGC 604 in M33, 30 Dor in the LMC, and the regions in NGC 2403. The linear size of the largest H II regions in Sc, Sd, and Sm galaxies appears to be a steep function of galaxian absolute magnitude.

Besides the extended H II regions, Baade began a search for unresolved "stellar" nebulosities. Two were found by blinking the 103a-E + RG1 plate with a 103a-D + GG11 plate, and are marked as objects A and B in Figure 13.

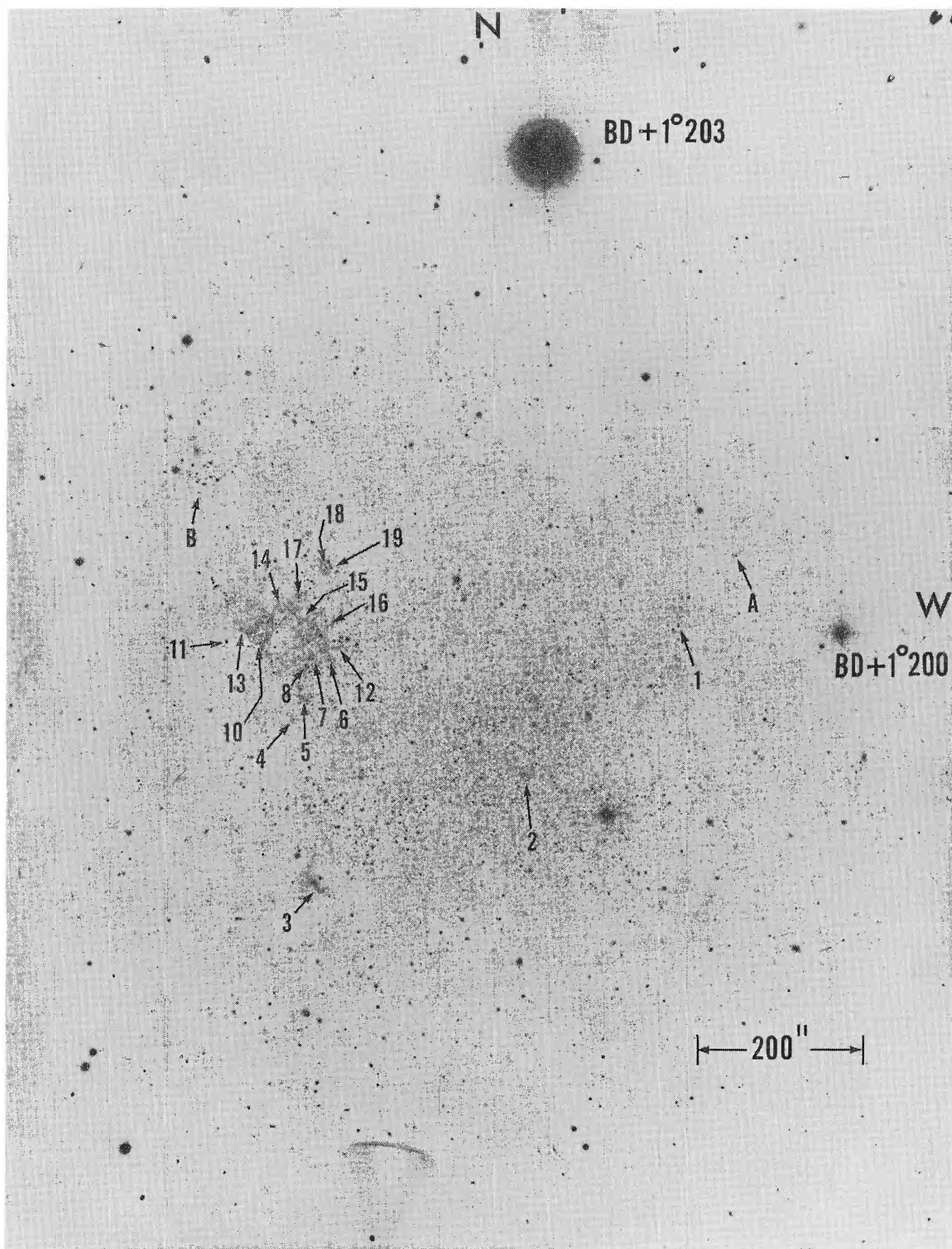


FIG. 13.—Identification chart for the H II regions from a 103a-E + RG1 plate taken with the 200-inch Hale reflector.

SANDAGE (*see* page 31)

PLATE 8

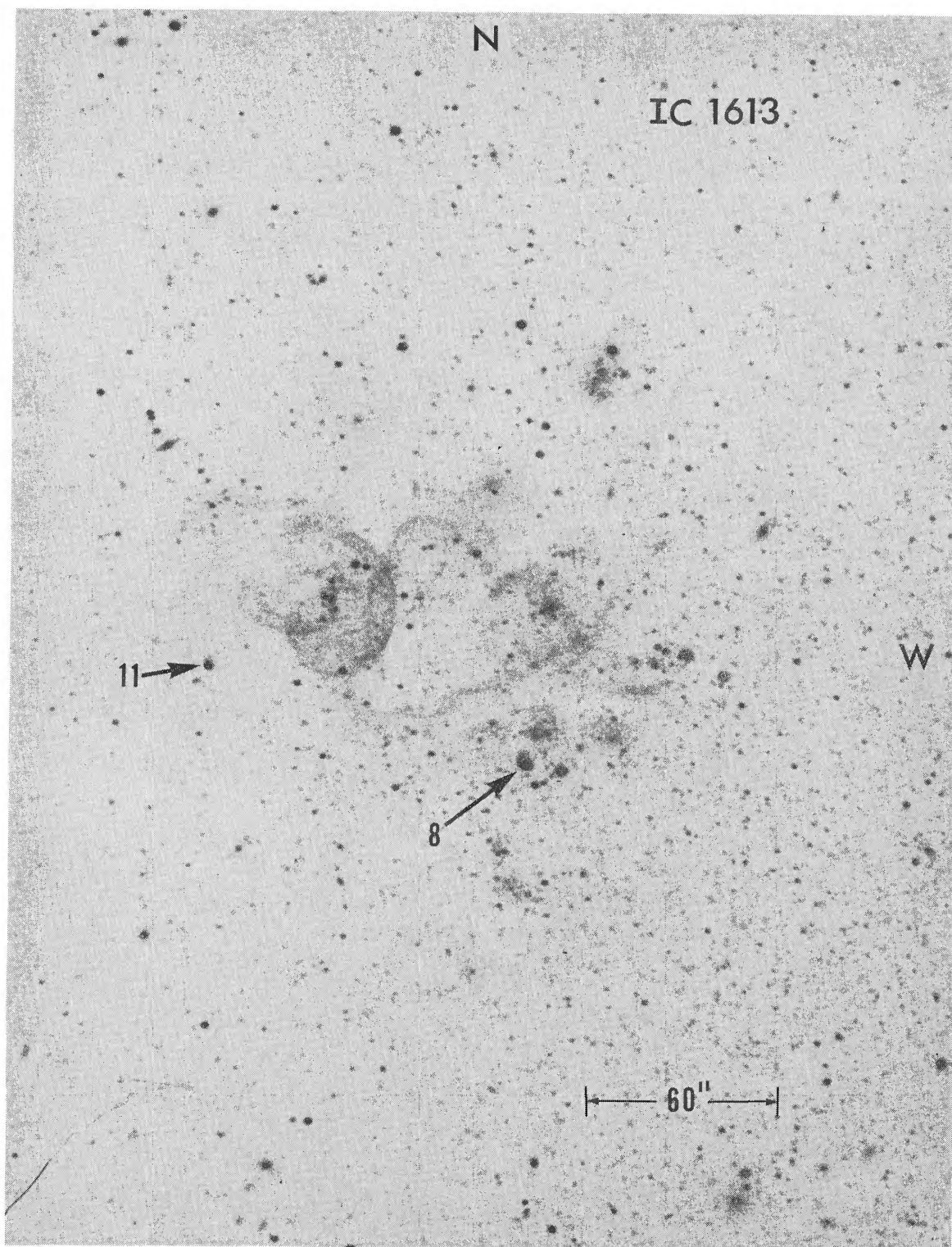


FIG. 14.—Enlarged portion of the NE quadrant of Fig. 13

SANDAGE (see page 31)

VII. ANGULAR EXTENT OF THE GALAXY

Baade took a series of deep red plates to search for the extent of the background sheet of Population II stars, which begins suddenly to resolve into stars at $V \simeq 21.5$. The series of 200-inch plates was centered to map the boundary on the East, South, and West sides adequately, as marked on the reproduction from a blue 48-inch Schmidt plate shown in Figure 15 (Plate 9).

The limiting boundary is roughly elliptical, with major and minor axes of $25'.07$ and $20'.27$, respectively, at a position angle of about 90° . The linear dimensions are 5600 by 450 pc, which represent the extreme size to which the oldest stars can be traced. Figure 15 shows that the prominent Population I component is confined well within these boundaries by about a factor of 2. IC 1613 is an exceedingly small galaxy.

VIII. REMAINING OPTICAL PROBLEMS

The preceding reconnaissance study can be extended in several ways. Of most immediate concern is a test between the interpretations of Figures 11 and 12. This can be done by obtaining light curves for the faint TBD variables in Table 1, and by measuring all the variables on a series of 103a-D + GG11 plates for color indices. Because V -magnitude standards exist for many sequence stars (Table A2 of the Appendix), the task is not large once an adequate series of yellow plates is available.

The color-magnitude diagram to $V \simeq 22$, together with the luminosity function for main-sequence and supergiant red stars, would provide an important comparison of evolutionary lifetimes of supergiants and Cepheids.

First plates to obtain the C-M diagram have been measured by Katem, but the program is not now complete.

It is a pleasure to thank Basil Katem for his help in the long and tedious task of reducing all data to the new magnitude system, and in measuring the areas of the light curves to obtain mean intensities. It is also a pleasure to thank Felice Woodworth for her excellent preparation of the illustrations for press, and Judy Harstine for the difficult work of typing Table 2. I am most grateful to Henrietta Swope for critically reading the manuscript.

APPENDIX

THE ADOPTED SCALE AND ZERO POINT
OF THE MAGNITUDE SYSTEM

A. SANDAGE, BASIL KATEM, AND ANN H. MATTHEWS

Photoelectric UBV measurements of thirty-eight stars in and near IC 1613, measured at the 200-inch prime focus, are listed in Table A1. Stars fainter than $V = 19.3$ were centered in the photometer diaphragm by blind-offset techniques. A sky-blocking diaphragm of $7''.6$ diameter was used in all cases. The listed stars have been identified in Figure 1.

Stars of the photoelectric sequence brighter than $V = 17.5$ are undoubtedly foreground. Seven of these have adequate $U - B$, $B - V$ data to estimate the reddening. Because of the high latitude ($b = -61^\circ$), some mild intrinsic ultraviolet excess is expected for those foreground stars in the near halo. The excess is present for stars T, H, and 17, but the effect on the reddening determination is minor. The data require $E(B - V) \leq 0.03$, and it could be zero. In any case, it is almost certainly smaller than the $E(B - V) = 0.07$ which is predicted from the cosecant law with a "standard" reddening half-thickness of $E(B - V) = 0.06$ mag. IC 1613 is, then, another example of low reddening in the pole for individual objects as shown by the high-latitude globular clusters (Sandage 1969), by E galaxies (Peterson 1970), and by NGC 2403, for example (Tammann and Sandage 1968).

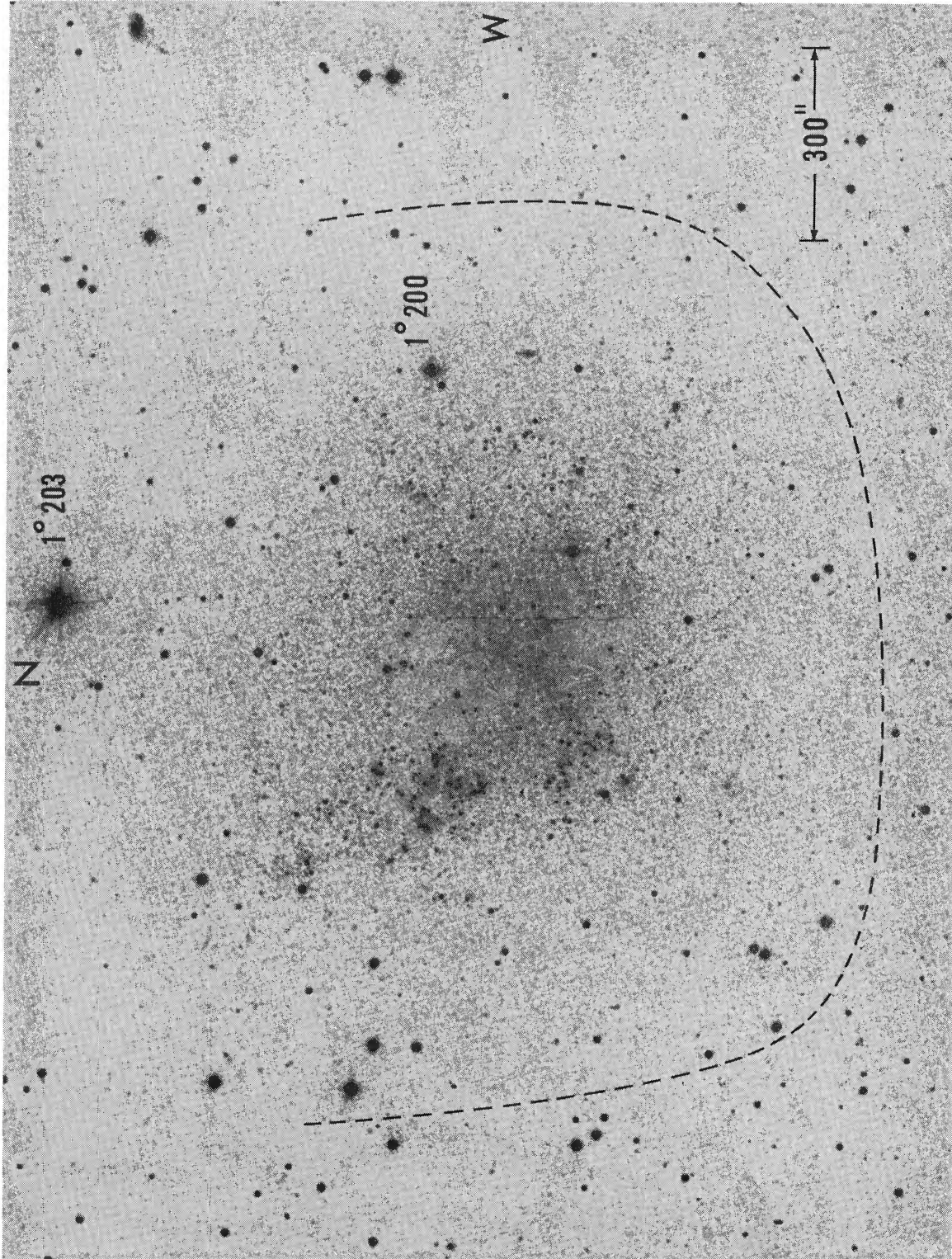


FIG. 15.—Enlarged copy of the blue plate of IC 1613 from the *Palomar Sky Survey*. The extent of the Population II component of the galaxy is marked as found from red 200-inch plates taken of the E, S, and W sectors.

SANDAGE (see page 32)

Extensive photographic smoothing was done on the photoelectric data so that the crowding problem could be statistically overcome. The results are shown in the final column of Table A1, and are plotted in Figure A1. There seems to be little difficulty brighter than $B \simeq 20.8$, but fainter than this the scatter becomes larger, and it seems clear that accuracies of ± 0.1 mag have not yet been reached for the faintest stars. However, no gross random errors larger than ± 0.2 mag appear to exist to the limit of the data at $B \simeq 21.7$.

The area of good definition on 100-inch 5×7 -inch plates is considerably smaller than the angular extent of IC 1613. Because it was crucial to place all secondary sequence stars on a homogeneous magnitude system, Baade took a series of plates at different centers over the face of IC 1613 so that the areas of good definition overlapped. He did this initially with 100-inch plates, and later with 5- and 15-minute exposures with the 200-inch. Under his direction, these overlapping plates were measured with an iris diaphragm photometer by Mrs. Matthews so that all sequence stars could be tied to a single system. Correlation curves were drawn for all stars in the overlap regions, thereby permitting reduction of all readings to a single plate. A final list of mean iris readings was produced.

TABLE A1
PHOTOELECTRIC SEQUENCE IN IC 1613

Star	V	B	$B-V$	$U-B$	n	B_{pg}
B.....	10.97	11.58	+0.61	+0.16	16	...
T.....	13.71	14.31	+0.60	+0.01	2	...
G.....	13.72	14.50	+0.78	+0.42	1	...
A.....	14.24	14.98	+0.74	+0.29	3	...
H.....	14.58	15.11	+0.53	-0.04	1	...
C.....	14.74	15.55	+0.81	+0.40	1	...
26.....	16.40	17.60	+1.20	+1.17	2, 1	17.58
17.....	16.42	16.96	+0.54	-0.05	2	16.99
28.....	17.02	18.39	+1.37	...	1	18.46
24.....	17.23	17.86	+0.63	...	1	17.73
Q.....	18.22	18.25	+0.03	-0.50	2, 1	18.20
L.....	18.56	18.36	-0.20	-0.84	1	18.21
M.....	18.57	18.43	-0.14	-0.72	1	18.27
14.....	18.86	18.55	-0.31	-1.02	1	18.47
5.....	18.91	18.66	-0.25	-1.05	1	18.53
44a.....	18.96	19.86	+0.90	+0.76	2, 1	19.96
18c.....	19.24	21.21	+1.97	...	1	20.85
19a.....	19.26	19.25	-0.01	...	1	19.26
53a.....	19.32	21.28	+1.96	...	1	20.79
P.....	19.78	19.82	+0.04	+0.21	1	...
29.....	19.86	19.73	-0.13	-0.15	1	19.70
19d.....	20.12	20.33	+0.21	+0.06	1	20.32
24f.....	20.21	21.62	+1.41	...	1	21.55
13d.....	20.40	21.49	+1.09	...	V1, B2	21.65
9c.....	20.52	21.02	+0.50	...	1	21.05
13c.....	20.56	20.88	+0.32	...	1	21.15
47c.....	20.63	20.89	+0.26	...	1	21.00
19e.....	20.65	20.56	-0.09	...	1	20.48
13b.....	20.71	20.65	-0.06	...	2	20.90
45e.....	20.73	20.64	-0.09	...	1	20.75
12d.....	20.78	21.68	+0.90	...	2	21.69
13a.....	20.93	20.74	-0.19	(-0.81)	1	20.75
17b.....	20.93	20.64	-0.29	...	1	20.67
24d.....	20.98	21.49	+0.52	...	1	21.30
37e.....	21.22	21.26	+0.04	...	1	21.19
14e.....	21.49	21.08	-0.41	(-1.36)	1	20.95
A5.....	21.53	21.52	-0.01	(-0.86)	1	21.33
24c.....	21.70	21.26	-0.44	(-1.29)	1	21.00

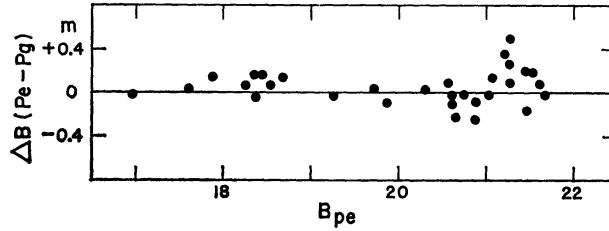


FIG. A1.—Comparison of the photoelectric and photographically smoothed primary stars sequence listed in Table A1.

TABLE A2
ADOPTED MAGNITUDES OF COMPARISON STARS

Star	B	(B-V)	Star	B	(B-V)	Star	B	(B-V)	Star	B	(B-V)	Star	B	(B-V)
1/3/14			13a	20.75	-0.07	24a	20.29	0.11	37a	20.28	+0.08	47b	20.55	.1.39
a	20.03	-0.10	b	20.90	0.13	b	20.77	0.07	b	20.60	0.32	c	21.04	0.28
b	20.23	0.12	c	21.15	c	21.00	-0.12	c	20.83	-0.49	c'	20.91	-0.34
c	20.51	0.59	d	21.65	1.47	d	21.30	0.52	d	21.01	0.32	d	21.37
d	20.85	0.44	e	21.80:	e	21.52	e	21.19	0.35	d'	21.44
e	20.95	0.28	15a	20.31	0.00	f	21.55	1.35	f	21.45	e	21.79
f	21.10	0.38	b	20.56	0.19				38a	18.10	-0.09	48a	21.20	0.04
g	21.45	c	20.91	0.07	25/50			b	18.55	-0.41	b	21.35	0.30
h	21.90	d	21.25	0.20	a	20.00	1.01	c	18.86	-0.5	c	21.47	0.47
2/19			d'	21.25	b	20.24	0.08	d	19.26	-0.4	d	21.64
A	18.20	0.10	e	21.64	c	20.40	0.22	e	19.11	-0.47	e	21.90
a	19.28	-0.15	16a	19.91	0.32	d	20.74	0.47	f	19.78	0.09			
b	19.70	-0.11	b	20.34	-0.09	e	20.98	-0.52				51/59A	21.01	1.24
c	19.91	-0.15	c	20.71	-0.25	f	21.45	0.43	39/56			a	20.72	0.22
d	20.31	0.27	c'	20.48	0.22	g	21.78	A	19.13	1.87	a	21.14	1.35
e	20.46	0.15	d	21.11	-0.27	26/27/63			a	18.90	0.75	b	21.37
f	20.78	-0.12	d'	21.04	-0.07	A	20.27	0.12	b	19.25	0.04	c	21.58
g	21.08	-0.22	e	21.23	0.15	a	20.43	0.18	c	19.56	0.17	d	21.74
6a	20.12	0.26	f	21.39	b	20.68	0.29	d	19.97	0.20	52a	20.42	0.22
b	20.50	0.43	17/36			c	20.94	40/49			b	20.67	0.31
c	21.16	-0.35	a	20.20	0.35	c'	21.44	a	20.73	-0.12	c	21.08
d	21.30	b	20.67	0.26	d	21.38	b	20.90	-0.42	d	21.32
e	21.51	c	20.89	-0.14	e	21.62	c	21.08	e	21.50
f	21.65	d	21.34	e'	21.68	e	21.35	53A	20.70	0.10
7/52			e	21.66	f	21.83	f	21.70	a	20.79	1.77
a	20.42	0.25	f	21.85	28A	20.74	0.18	g	21.80	b'	21.13	0.08
b	20.66	0.32	18a	20.16	-0.21	a	21.15	0.55	h	22.0:	b	21.10	0.93
c	21.08	b	20.42	-0.15	c	21.37	1.53	41a	21.02	0.90	c	21.18	0.26
d	21.32	c	20.85	1.66	d	21.65	b	21.25	d	21.38
e	21.50	c'	20.83	-0.03	e	21.91:	c	21.40	e	21.69
8a	20.67	0.53	d	21.30	e'	21.87	d	21.85	e'	21.75:
b	21.14	-0.05	e	21.35	29a	21.10	e	22.0:	54a	20.78	-0.47
c	21.34	f	21.65	b	21.48	42a	18.70	-0.50	b	21.08	0.06
d	21.65	20a	18.78	-0.23	c	21.70	b	18.66	-0.49	c	21.26
9b	20.73	0.33	b	18.94	0.35	d	21.89	c	19.13	-0.08	d	21.60
c	21.05	0.61	b'	19.76:	30A	20.40	0.13	d	19.41	-0.31	e	21.72:
d	21.30	0.51	c	19.83	-0.05	a'	20.64	-0.02	e	19.85	-0.14	57a	20.98	0.18
e	21.76:	d	19.90	-0.12	b	20.98	-0.15	43a	18.56	-0.65	b	21.25
e'	21.77:	d'	20.09	0.06	c	20.99	-0.11	b	19.17	0.00	c	21.50
10a	20.36	0.06	e	20.59	0.12	d	21.48	0.88	c	19.43	-0.27	d	21.52
b	20.77	-0.06	e'	20.29	0.07	e	21.53:	d	19.76	-0.12	e	faint
c	21.03	f	20.91	0.03	f	21.62:	e	20.02	-0.09	60a	21.03	-0.12
d	21.45	21γ	20.50	-0.02	31/58			f	20.32	-0.09	b	21.22	0.06
e	21.65	b	20.78	-0.01	a	19.32	-0.35	44A	19.81	0.13	c	21.25	0.45
11A	18.47	-0.58	22A	17.00	-0.15	45a=b	19.73	-0.16	a	19.96	1.04	d	faint
a	19.80	-0.06	a	17.91	-0.26	c	20.46	-0.20	b	19.96	0.14	61a	20.91	-0.01
b	19.88	-0.19	b*	18.19	d	20.94	-0.66	c	20.11	0.35	b	21.31
c	20.10	0.16	c	18.93	-0.44	32a	18.62	-0.48	d	20.39	0.49	c	21.46	0.39
d	20.50	-0.19	d	19.31	-0.40	b	19.44	-0.14	e	20.74	0.52	d	21.67
e	20.73	-0.44	e	19.93	-0.08	c	19.90	-0.21	45a	19.73	-0.16	e	21.75:
f	20.82	1.45	f	20.35	-0.11	d	19.95	-0.24	b	20.21	-0.03	62a	20.90	-0.14
g	21.21	0.17	g	20.60	-0.16	34a	20.49	+0.49	c	20.50	-0.21	b	20.92	-0.44
12a	20.80	-0.25	23A	18.64	-0.24	b	20.82	-0.08	d	20.57	0.05	c	20.88	0.13
b	21.00	0.34	a	18.87	-0.11	c	21.16	+0.37	e	20.75	0.19	d	21.43	1.08
c	21.39	0.14	b	19.57	-0.15	d	21.53	46a	21.09	e	21.68
d	21.69	b'	19.58:	-0.17	e	21.96	b	21.21			
e	21.89	c	19.92	0.00	35a	21.19	c	21.60			
e'	21.80	d	20.4:	0.12	b	21.19	-0.07	d	21.67	1.16			
			e	20.54	0.12	c	21.38	e	faint			
			f	20.73	1.80	d	21.67						
						e	21.77						
						f	21.9:						

Stars for the photoelectric sequence were chosen from this list. All that was then required was to draw calibration curves of B_{pe} versus iris values for the primary standards, from which magnitudes of all secondary stars were then determined.

Four complete series of overlapping 200-inch plates were measured and reduced in this way. The series were (a) 5-minute exposures behind a Schott GG1 filter, (b) 5-minute exposures behind a GG13, (c) 15-minute exposures behind a GG1, and (d) special measurements by Katem for a separate program on the color-magnitude diagram in which a number of the secondary standards were carried as unknowns. After applying a color equation to the two GG1 series to reduce them to the GG13 system, all four series were averaged for each star to form the adopted B -magnitude system for the sequences.

A special series of yellow plates (103a-D + GG11) was measured by Katem to obtain *preliminary* V magnitudes. The weight of these is considerably less than for the blue magnitudes (which depend on four series, each series consisting of about five plates), but they are useful at this stage as an indication of $B - V$ color.

The final data for 279 stars are listed in Table A2, which is, in a sense, more fundamental than Table A1 because all values in Tables 2, 3, 4, 5, and 6 depend directly on it. Future work to improve the magnitude scale will aim at improving Table A2.

REFERENCES

- Adams, W. S., and Joy, A. E. 1918, *Proc. Nat. Acad. Sci.*, **4**, 129.
 Arp, H. C. 1960, *A.J.*, **65**, 404.
 Baade, W. 1928, *Astr. Nach.*, **234**, 407 (Nr. 5612).
 ———. 1944, *Ap. J.*, **100**, 137.
 Baade, W., and Swope, H. H. 1963, *A.J.*, **68**, 435.
 ———. 1965, *ibid.*, **70**, 212.
 Christy, R. F. 1970, *J.R.A.S. Canada*, **64**, 8.
 Dickens, R. J., and Carey, J. V. 1967, *R.O.B.*, **No. 129**, E335.
 Gaposchkin, C. P., and Gaposchkin, S. 1966, *Smithsonian Contr. Ap.*, **9**, 1.
 Gascoigne, S. C. B. 1969, *M.N.R.A.S.*, **146**, 1.
 Gascoigne, S. C. B., and Kron, G. 1965, *M.N.R.A.S.*, **130**, 333.
 Gent, H. van. 1933, *B.A.N.*, **7**, 21.
 Hertzsprung, E. 1926, *B.A.N.*, **3**, 115.
 Holmberg, E. 1950, *Medd. Lund Astr. Obs., Ser. II*, No. 128.
 Hubble, E. P. 1925, *Ap. J.*, **62**, 409.
 Hubble, E., and Sandage, A. 1953, *Ap. J.*, **118**, 353.
 Kayser, S. E. 1967, *A.J.*, **72**, 134.
 Kukarkin, B. V., Parenago, P. P., Efremov, Yu. I., and Kholopov, P. N. 1957, *General Catalog of Variable Stars* (2d ed.; Moscow: Academy of Sciences of U.S.S.R. Press).
 Merrill, P. W., and Wilson, R. E. 1942, *Ap. J.*, **95**, 248.
 Mohr, J. 1938, *Pop. Astr.*, **46**, 379.
 Osvalds, V., and Risley, A. M. 1961, *Pub. Leander McCormick Obs.*, **11**, Part 21, 147.
 Peterson, B. 1970, *A.J.*, **75**, 695.
 Plaut, L. 1964, in *Stars and Stellar Systems*, Vol. 5, *Galactic Structure*, ed. A. Blaauw and M. Schmidt (Chicago: University of Chicago Press), p. 267.
 Sandage, A. 1958, *Ap. J.*, **127**, 513.
 ———. 1962, in *Problems of Extragalactic Research*, ed. G. C. McVittie (New York: Macmillan Co.), p. 359.
 ———. 1969, *Ap. J.*, **157**, 515.
 Sandage, A., and Tammann, G. A. 1968, *Ap. J.*, **151**, 531.
 ———. 1969, *ibid.*, **157**, 683.
 ———. 1971, in preparation.
 Seares, F. H., Kapteyn, J. C., and van Rhijn, P. J. 1930, *Mount Wilson Cat. Photographic Mags. in Selected Areas 1-139* (Washington: Carnegie Institution of Washington).
 Smak, J. I. 1966, *Ann. Rev. Astr. and Ap.*, **4**, 19.
 Stebbins, J., Whitford, A. E., and Johnson, H. L. 1950, *Ap. J.*, **112**, 469.
 Tammann, G. A., and Sandage, A. 1968, *Ap. J.*, **151**, 825.
 Gent, H. van. 1933, *B.A.N.*, **7**, 21.
 Wolf, M. 1906, *M.N.R.A.S.*, **67**, 91.
 Woolley, R. v. d. R., Sandage, A., Eggen, O. J., Alexander, J. B., Mather, L., Epps, E., and Jones, S. 1962, *R.O.B.*, **58**, E31.

